Step-Bunching Transitions on Vicinal Surfaces and Quantum N-mers

V. B. Shenoy[1], Shiwei Zhang[2] and W. F. Saam[3]
[1]Division of Engineering, Brown University, Providence, RI 02912.
[2] Department of Physics and Department of Applied Science, College of William and Mary, Williamsburg, VA 23187.
[3] Physics Department, The Ohio State University, Columbus, OH 43210.
(February 1, 2008)

We study vicinal crystal surfaces within the terrace-step-kink model on a discrete lattice. Including both a short-ranged attractive interaction and a long-ranged repulsive interaction arising from elastic forces, we discover a series of phases in which steps coalesce into bunches of n_b steps each. The value of n_b varies with temperature and the ratio of short to long range interaction strengths. For bunches with large number of steps, we show that, at $T = 0$, our bunch phases correspond to the well known periodic groove structure first predicted by Marchenko. An extension to $T > 0$ is developed. We propose that the bunch phases have been observed in very recent experiments on Si surfaces, and further experiments are suggested. Within the context of a mapping of the model to a system of bosons on a 1D lattice, the bunch phases appear as quantum n-mers.

I. INTRODUCTION

The study of the equilibrium properties of a stepped vicinal crystal surface is important from technological and fundamental perspectives. The understanding of the surface morphology is key to phenomena like epitaxial growth, chemical etching and catalysis. In addition, it also provides a fascinating example of a problem which has a much broader context, reaching, via a mapping onto a one-dimensional quantum chain, into the realm of 1D quantum liquids. In this paper we consider the morphology of vicinal surfaces in the case where step-step interactions are repulsive at large separations and attractive at short distances. Our work is aimed at explaining the features of the surface morphology of miscut Si (113) surfaces observed in two sets of experiments. The first is that that of the description of apparent tricritical phenomena observed in a beautiful set of experiments by Song *et al.* [1–3] on silicon surfaces oriented between the (113) and (114) crystalline directions. The second is the very recent observations of multiple-height steps by Sudoh *et al.* [4] on vicinal (113) surfaces misoriented towards a low symmetry azimuth which is directed 33^0 away from the $[\bar{1}10]$ direction towards the $[\bar{3}\bar{3}2]$ direction.

Recent theoretical work [5,6] attempted to explain the experiments of Song *et al.* in terms of a continuum model of steps interacting via a long-ranged repulsive elastic interaction and a short-ranged attractive interaction. This model produces a tricritical point but requires somewhat artificial tuning to give the observed coexistence curve exponent and fails to describe the observed bunching of steps on the vicinal surfaces coexisting with the (113) facet. Furthermore, the experimental system seems to be very close to or in the region where the renormalization group method that is used to study the model fails. Here we explore the consequences of retaining the discrete, atomic nature of steps on a crystal surface within the same model. We discover entirely different physics. The steps do not phase separate but instead can coalesce into bunches whose size depends on the relative strengths of the short- and long-range interactions and temperature. Vicinal surface phases can be characterized by widely separated n-bunches and transitions occur between phases having different values of n. We propose that bunch phases with large n correspond to the two-phase coexistence region of Song *et al* and that the n=2,3,4 bunch phases produce the multiple-height steps seen by Sudoh *et al.* For bunches with large number of steps, we show that, at $T = 0$, our bunch phases correspond to the well known periodic groove structure predicted by Marchenko [7]. While Marchenko's calculations are valid only at $T = 0$, our theory predicts the evolution of the periodic groove structure as the temperature of the surface is raised. In addition, we show that Marchenko's phenomenological parameters like the edge energy can be determined in terms of the parameters that characterize the long and short range step-step interaction strengths. The physics of bunching transitions that we study here is very different from the recently studied step bunching due to applied stress, electromigration and other kinetic effects [12]. In our case, the bunching transitions occur in an equilibrium setting due to competing interactions acting on different length scales. The relevance of the bunching transitions described here go well beyond the crystal surface problem. In particular, the model provides opportunities to study many-body phenomenon arising from coupling of modes on different length and energy scales. A brief description of this work has already been reported [8].

The model we use is the terrace step kink model (TSK) [9]. This lattice model can be mapped onto an equivalent quantum mechanical model of interacting spin-less fermions or hard-core bosons. Details are found in earlier work [9–11]. In the quantum picture it is well-known that the 1-bunches form a Luttinger lattice liquid. Our results generalize this picture to a Luttinger lattice liquid which can form dimers (the 2-bunches), trimers (the 3-bunches),

and in general n-mers. The transitions between these phases are quantum many-body phenomena of a type hitherto unexplored. In the following section, we introduce the TSK model and develop the mapping to the hard core boson problem. In Section III, we analyze the model in what we call the extreme dilute limit (EDL), where bunches are widely separated. For $T = 0$, the exact solution clearly reveals the essence of our problem, a series of first-order bunching transitions. For bunches with large numbers of steps, we show the connection between the bunches phases and the periodic groove structure predicted by Marchenko [7]. In the same EDL, using exact diagonalization on small systems to reveal the nature of the bunching transitions, we develop the physics for $T > 0$. Section IV uses phenomenology coupled with scaling arguments to include interactions between bunches in the case that they are widely separated and to study the effects of the interactions on transitions from one bunch size to another. In Section V we use Quantum Monte Carlo simulations to check the results of exact diagonalization by explicitly looking at particle-particle correlations through a series of bunching transitions. Section VI applies our results to crystal shapes. Section VII gives a detailed comparison of our results with continuum theories. In Sec.VIII we compare the key experimental findings with the predictions of the theory. Differences and similarities are highlighted, and directions for further development of the theory are suggested. We conclude by discussing the main results and pointing directions of future research.

II. HAMILTONIAN OF INTERACTING STEPS

In order to study the thermodynamics of surfaces that are miscut by a small amount from a reference surface, we will first derive the surface free energy by treating the miscut angle and temperature as thermodynamic variables. The surface free energy will be expressed in terms of the ground state energy of a one-dimensional quantum mechanical model that will be derived using transfer matrix methods. In the study of interacting steps it is common to use both discrete and continuum models. In this section we introduce the TSK lattice model and the equivalent quantum mechanical model. We do not go into all the details of the derivation, but refer the reader to earlier work [9]. We then compare the kink energy in the lattice model to the step-stiffness in the continuum model. It turns out that it is important to understand the limiting process which brings out the equivalence of the two models. While it is generally true that when the limiting process is carried out properly, it is possible to switch between the models, caution should be exercised against making erroneous conclusions about one model based on the results of the other. The bunching transition is one such example, where the cut off distance (lattice spacing) in the lattice model plays a crucial role. As we discuss in Sec. VII, there is nothing corresponding to bunching transitions in the continuum model; they are purely lattice effects. On the other hand, to study the interactions between steps whose average separation is much larger the lattice spacing, one can use either the lattice model or the continuum model. We will now turn our attention to the TSK model and (1) derive the quantum hamiltonian in terms of hard-core boson operators, (2) make the connection between the free energy of the surface to the ground state energy of the quantum mechanical system and (3) derive the connection between the kink energy in the lattice model and step stiffness in the continuum model.

A. Terrace Step Kink Model

Let us consider a square lattice with M rows and L columns as shown in Fig. (1), where steps between terraces are specified by bonds on this lattice. Let the steps in the TSK model run parallel to the y-axis, so that the slope of the crystal face is in the x-direction. One can specify a configuration of this system by specifying the x-coordinates of each of the N steps at each of the y-coordinates. The lattice spacing in the x and y direction is denoted by a_x and a_y respectively. The density of steps is related to the slope of the interface under consideration through the relation $s = tan(\theta) = (Na_z/La_x)$ where a_z is the lattice parameter in the z-direction or the step height. For notational convenience we specify a configuration by the state vector $|x_1, x_2, ..., x_N\rangle_k$, where x_j denotes the position of the jth step in the kth row. The position of the step can only change by ± 1 between the rows by creating a kink. The transfer matrix describes the propagation of steps from row to row. It can be determined by a kink energy Γ, an energy η_0 for a unit length of the straight step, and an interaction energy V_{ij} between parallel straight pieces of steps labeled i and j. To render interactions between different rows (steps interacting at different values of y) tractable, we treat them in an average way: we compute V_{ij} as the interaction between a unit length of step at i and an infinite straight step at j. We expect this approximation to preserve the qualitative physics of interest here. In going from row k to row $k+1$, if the ordinates of p steps are unchanged while the other $(N-p)$ steps change by ± 1, then the transfer matrix element has a contribution $\exp\left(-\beta a_y N\eta_0 - \beta\Gamma(N-p)\right)$, where $\beta = 1/k_B T$. The matrix element vanishes if $x_i = x_j$ for $i \neq j$, i.e. the steps do not cross. The transfer matrix element also has a multiplicative element contribution from the step interactions, that can be written as $\exp\left(-\beta a_y \sum_{i<j} V_{ij}\right)$. A convenient operator representation is obtained

by associating a step creation operator $a_j^\dagger$ for a step at x_j in row k: $a_j^\dagger a_j$ denotes a straight step while $a_{j+1}^\dagger a_j$ and $a_j^\dagger a_{j+1}$ denote a kink to the right and to the left, respectively. The a's are defined so that $(a_j^\dagger)^2 = 0$, which imposes the non-crossing condition. This gives us a choice of a fermionic or hard-core bosonic representation of a's. We adopt the hard-bosonic representation, where a's satisfy the usual bosonic commutation relations

$$[a_i, a_j] = \left[a_i^\dagger, a_j^\dagger\right] = \left[a_i, a_j^\dagger\right] = 0 \tag{1}$$

when $i \neq j$ and satisfy anti-commutation relations on the same site, *i.e.,*

$$[a_i, a_i]_- = \left[a_i^\dagger, a_i^\dagger\right]_- = 0, \;\; \left[a_i, a_i^\dagger\right]_- = 1. \tag{2}$$

The onsite anti-commutation relations take care of the hardcore condition $(a^\dagger)^2 = 0$. This representation is equivalent to the fermion representation introduced in Ref. [9]. The fermion operators that anti-commute on different sites are related to the hard core boson operators through the unitary Jordan-Wigner transformation [13].

Let us denote the $(N \times N)$ transfer matrix by $\hat{\mathcal{T}}$. For mathematical convenience we take the continuum limit in the y-direction (i.e. we take the limit of the lattice spacing $a_y \to 0$). In this limit to first order in a_y the transfer matrix can be written as

$$\hat{\mathcal{T}} = \hat{1} - \frac{a_y}{k_B T}\hat{H}, \tag{3}$$

where $\hat{1}$ is the identity operator and the quantum hamiltonian is defined as

$$\hat{H} \equiv \eta(T)\sum_i n_i - t\sum_i \left[a_{i+1}^\dagger a_i + a_{i+1}a_i^\dagger - 2n_i\right] + \sum_{(i,j)} V_{ij} n_i n_j. \tag{4}$$

where (i,j) is used to denote a sum over distinct pairs of bosons, $n_i = a_i^\dagger a_i$, and the free energy of a straight step $\eta(T) = \eta_0 - 2t$, where the hopping parameter t is defined as

$$t = \lim_{a_y \to 0} \frac{\exp\left(-\beta\Gamma\right)}{\beta a_y}. \tag{5}$$

It should be noted that the kink energy Γ is a function of a_y and diverges in the limit of vanishing a_y, but the ratio given by Eq. (5) remains finite. Note that since t is a monotonically increasing function of T which vanishes as $T \to 0$, t itself serves as an effective temperature variable.

The eigenvalues of the transfer matrix can be related to the projected surface energy of the miscut surface through the relation [9]

$$f(s) = \frac{\gamma(s)}{cos(\theta)} = \gamma_0 - \frac{k_B T}{M L a_x a_y}\log\left(Tr\left[\hat{\mathcal{T}}^M\right]\right), \tag{6}$$

where γ_0 is the surface tension of the reference surface and $\gamma(s)$ is the free energy per unit area of the miscut surface i.e. the surface tension. In the continuum limit where Eq. (3) is satisfied, the projected free energy can be related to the ground state energy $E_0\left[N,T\right]$ of $\hat{H}$ through

$$f(s) = \gamma_0 + \frac{E_0\left[N,T\right]}{L a_x}. \tag{7}$$

This relation can be used to relate the physical properties of the surface like the curvature, stiffness etc. to the ground state energy of the hard-core boson system. We now turn to a discussion of the form of the step-step interactions that will enable us discuss the physics of faceting transitions.

B. Step-Step Interactions

In this paper we consider step-step interactions consisting of a repulsive long range part and an attractive short range part. We write the inverse square long range part in the form

$$V_{i,j}^{lr} = \frac{G}{|i-j|^2} \ , \tag{8}$$

and the short range part as

$$V_{i,j}^{sr} = -\sum_{k=1}^{n_s} U_k \delta_{|i-j|,k} \ , \tag{9}$$

where δ is the usual kronecker delta. The quantity G has contributions arising from the elastic interactions as well as from the electronic charge rearrangements along the steps [9]. The elastic part depends on the elastic constants of the crystal; for isotropic crystals it has the form [14,15]

$$G = 2\frac{(1-\sigma^2)\vec{f}^2}{\pi E a_x^2}, \tag{10}$$

where E and σ are the Young's modulus and Poisson's ratio respectively and $\vec{f}$ is the strength of the vector surface dipole force at a step. In general for non-metallic crystals the electronic rearrangements along the steps can be ignored, and $G > 0$. In the case of metallic crystals, G can have either sign depending on the details of the electronic charge rearrangement along the steps. The short range potential depends on the details of the step-step interactions on atomic scales and has to be worked out from a microscopic calculation. There is ample experimental evidence [1–3,16,17] that this quantity can be attractive, *i.e.* $U_k > 0$, on a few lattice spacings from the step [18]. The purpose of this paper is to explore the phases of vicinal surfaces and the associated crystal shapes in crystals with $G > 0$ and $U_k > 0$. In the remainder of the paper we will consider the case $n_s = 1$ and $U_1 \equiv U$, though in Sec. VII we comment on the physics of systems with $n_s > 1$. For convenience, we re-scale the hopping strength to unity, so that the interaction parameters get scaled to $G \to g \equiv G/t$ and $U \to u \equiv U/t$, while the free energy per step is rescaled as $\hat{\eta}(T) = \eta(T)/t$. From this point on, we will focus on the rescaled Hamiltonian $\mathcal{H}$, written as

$$\mathcal{H} = \hat{\eta}(T)\sum_i n_i - \sum_i \left[a_{i+1}^\dagger a_i + a_{i+1}a_i^\dagger - 2n_i\right] + g\sum_{(i,j)}\left[\frac{1}{|i-j|^2} - \left(\frac{u}{g}\right)\delta_{|i-j|,1}\right] n_i n_j. \tag{11}$$

Note that g scales inversely with the effective temperature variable t.

C. Step Stiffness and Kink Energy

In the study of the thermodynamics of steps it is very common to use a continuum model, where the Hamiltonian of a single step with coordinate $y(x)$ is written as

$$H = \frac{\Sigma}{2}\int \left(\frac{dy}{dx}\right)^2 dx, \tag{12}$$

where Σ is the step stiffness. For a single step it is instructive to make the connection between the kink energy Γ in the lattice model and the stiffness Σ in the continuum model. To this end, in Appendix A we derive, within the lattice model, the free energy of the step. By comparing the energies of the continuum model and the lattice model, we see that the the step stiffness can be written as

$$\Sigma = \lim_{a_y \to 0} \frac{k_B T}{2a_x^2}\left(\frac{a_y}{\exp\left(-\beta\Gamma\right)}\right) = \frac{(k_B T)^2}{2a_x^2 t}. \tag{13}$$

It should be noted that the quantity in the brackets assumes a finite value in in the limit of vanishing a_y. The above equation is key in understanding the connection between the discrete and continuum models. We will return to this equation when we discuss the stiffness of step bunches.

III. PHASE DIAGRAM IN THE EXTREME DILUTE LIMIT

The form of the interaction that we have considered for the step interactions has competing components acting at different length scales. As noted before, we will focus on the case where there is an attractive potential on the

near neighbor site only i.e $n_s = 1$ and $U_1 \equiv U$. We now show that a number of features of this many body system can be inferred from exact diagonalization of small systems in conjunction with some simple analytical calculations. In the discussions to follow, we will present simple physical arguments to show that the for sufficiently attractive interactions, the steps on the surface rearrange themselves into bunches at low temperatures. At $T = 0$, where the entropic effects are unimportant, the bunch size is completely determined by the ratio of the strengths of the attractive and repulsive interactions i.e. U/G. With increasing temperature, the steps start peeling off from the bunches in a series of bunching transitions. In the extreme dilute limit (the details of which will be clear in the discussions to follow), we obtain a phase diagram that shows these bunching transitions as function of temperature.

A. Phase diagram at $T = 0$

Let us now consider the limit $u \to \infty$ and $g \to \infty$ but u/g finite, so that $t \to 0$, and the hopping part of the Hamiltonian Eq. (11) can be completely ignored. This corresponds to taking the zero temperature limit of the vicinal surface. In this limit, the energy of the system is obtained by minimizing the total potential energy, and depends on the single parameter U/G. A little reflection reveals that in the dilute limit, the minimum energy configuration for a given U/G consists of bosons in bunches of size n_b that are well separated from each other. In a bunch, the bosons sit next to one another. For a bunch of size n_b, the energy per boson is given by

$$\epsilon(n_b) \equiv \frac{E_0[N, T = 0, n_b]}{N} = \eta(0) - U\left[\frac{(n_b - 1)}{n_b}\right] + G\left[\frac{1}{n_b}\sum_{i=1}^{n_b-1}\frac{(n_b - i)}{i^2}\right] + O((N/L)^2), \tag{14}$$

where the term $O((N/L)^2)$ comes from bunch-bunch interactions and is small in the dilute limit. We call the limit in which the bunch interactions are completely ignored, the *"extreme dilute limit"*(EDL). A straightforward minimization of $\epsilon(n_b)$ in the EDL reveals the phase diagram shown in Fig. (2), where the circles marked on the U/G axis separate bunches that differ in size by one. With increasing U/G, the bunch size keeps increasing; for $U/G < 1$ the bunch size is 1, for $1 < U/G < 1.5$ the bunch size is 2, for $1.5 < U/G < 1.83$ the bunch size is 3, for $1.83 < U/G < 2.08$ the bunch size is 4 and so on. At the circles marked in Fig. (2) (i.e. at $U/G = 1, 1.5, 1.83, 2.08, ...$) there is a coexistence of bunches that differ in size by one. From the graphs of the energy per boson vs. U/G shown in Fig. (3) for different n_b's, we see that the slope at the points where these curves intersect are not the same. The $T = 0$ bunching transitions brought about by changing U/G can then be considered first order.

With increasing U/G, the spacing between the regions that differ in bunch size by one becomes smaller and smaller. For large U/G, Eq. (14) becomes

$$\epsilon(n_b) = \epsilon_\infty + \frac{\epsilon_e}{n_b} - \frac{G}{n_b}\ln n_b + O(\frac{1}{n_b^2}), \tag{15}$$

where $\epsilon_\infty = \eta(0) + G\zeta(2) - U$ is the energy per step in a large bunch, $\epsilon_e = U - G - GC$ is the energy associated with the ends of the bunch, and $C = 0.577$ is Euler's constant. Minimizing $\epsilon(n_b)$ in Eq. (15) with respect to n_b leads to a bunch size given by

$$n_b \approx 0.561 \exp(U/G), \qquad U/G \gg 1, \tag{16}$$

which indicates that bunch size diverges rapidly with increasing U/G.

The above simple calculation has shown that the steps split themselves into bunches in the EDL at $T = 0$. In the next subsection, we study the unbinding of the steps with increasing temperature in the EDL. First, however, we connect the result Eq. (16) for large bunches with earlier work of Marchenko [7].

For the case at hand, if elastic interactions are ignored, steps have only the short-ranged attractive interaction $-U$. Here there is a coexistence (see, *e.g.* [9]) between the flat, step-free facet and the facet formed when there are steps at each site. The latter facet is inclined at an angle $\theta_0 = tan^{-1}(a_z/a_x)$ with respect to the former. All facets with angles θ such that $0 < \theta < \theta_0$ are unstable and will decompose into coexisting facets with angles 0 and θ_0. Marchenko [7] showed that when elastic interactions are taken into account, facets with $0 < \theta < \theta_0$ become stable, being formed from an array of grooves as shown in Fig. (4). Each groove is composed of a step-free portion followed by a step bunch, in the terminology of this paper. In fact this "groove" phase looks just like a bunch phase with n_b large. It should then be possible to connect Marchenko's results with those of Eq. (15) in the limit, the EDL, where the bunches are widely separated. This corresponds to the case of small θ. Marchenko also assumes small θ_0, as will we in making the connection to his work. In terms of the geometry shown in Fig. (4), we have

$$n_b = \frac{L_g \sin\theta}{a \sin\theta_0} \approx \frac{L_g \theta}{a_x \theta_0}, \tag{17}$$

where L_g is the length of a Marchenko groove and $a = \sqrt{a_x^2 + a_y^2}$. The surface energy per unit area of the grooved surface is

$$\begin{aligned}
\gamma_g(\theta) &= \frac{\gamma_0 L_2 + \gamma(\theta_0) L_1}{L_g} \\
&\approx \frac{\gamma_0 (L_2 + L_1 \cos\theta_0 (1 + (\epsilon_\infty / \gamma_0 a_x))}{L_g} - \frac{G}{L_g} \ln(\frac{L_g \theta}{a^* \theta_0}) \\
&\equiv \gamma_0(\theta) - \frac{G}{L_g} \ln(\frac{L_g \theta}{a^* \theta_0}),
\end{aligned} \tag{18}$$

where

$$\gamma(\theta_0) = \gamma_0 \cos\theta_0 + \frac{\epsilon(n_b) n_b}{a_x}, \tag{19}$$

and

$$a^* = a_x e^{\epsilon_e / G}. \tag{20}$$

Eq. (18) is precisely Marchenko's [7] result in the EDL if G can be identified as

$$G = 2\frac{(1-\sigma^2)\vec{F}^2}{\pi E}, \tag{21}$$

in which F is the surface force acting at the ends of the bunch. Now, an expression for G was given in Eq. (10) in terms of $\vec{f}$, the strength of the vector surface dipole force at a step. To connect $\vec{F}$ with $\vec{f}$, note that the surface force density due to an array of steps with density $n(x)$ is given by

$$\vec{\mathcal{F}}(x) = \int \vec{f} \vec{\delta}'(x - x_0) n(x_0) dx_0 = \vec{f} \frac{dn(x)}{dx}. \tag{22}$$

$\vec{\mathcal{F}}(x)$ can be integrated to obtain the force $\vec{F}$ on the surface at the edge of a bunch. Noting that the step density has a discontinuity of size n_0, where $n_0 = (1/a_x)$ is the uniform step density in a bunch, we obtain

$$\vec{F} = \vec{f} \int \frac{dn(x)}{dx} dx = \frac{\vec{f}}{a_x}. \tag{23}$$

This result proves the equivalence of Eq. (21) to Eq. (10), and demonstrates that our theory is in fact a microscopic version of Marchenko's. In addition to connecting the surface force to the strength of the force dipole at the step, Eq. (20) gives an microscopic interpretation to the phenomenological edge energy, ϵ_e, in the Marchenko theory. Explicitly, in terms of the microscopic step interaction strengths, $\epsilon_e = U - 0.423G$.

Minimizing γ_g with respect to L_g at fixed θ and θ_0 gives

$$L_g = \frac{e a^* \theta_0}{\theta}, \tag{24}$$

which is Marchenko's result in the EDL and is equivalent to Eq. (16). At this minimum, we have

$$\gamma_g(\theta) = \gamma_0(\theta) - \frac{G\theta}{e a^* \theta_0}. \tag{25}$$

To further understand the grooved configuration, we make use of the relations $L_g \sin\theta = L_1 \sin\theta_0$ and $L_g \sin(\theta_0 - \theta) = L_2 \sin\theta_0$ to show that

$$\gamma_0(\theta) = \cos(\theta)[\gamma_0 + \frac{\epsilon_\infty}{a_x} \frac{\tan(\theta)}{\tan(\theta_0)}]. \tag{26}$$

The full projected free energy is, for small θ and θ_0, given by

$$f_g(\theta) = \frac{\gamma_g(\theta)}{\cos\theta} = \gamma_0 + (\frac{\epsilon_\infty}{a_x} - \frac{G}{ea^*})\frac{\theta}{\theta_0}. \tag{27}$$

The contribution to the projected free energy at $O(\theta^3)$ comes from bunch-bunch interactions that are ignored in the EDL. In the limit of vanishing θ that we are considering, the bunches interact via an inverse square interaction of strength Gn_b^2. A straightforward computation of the bunch interaction contribution yields

$$f_g(\theta) = \frac{\gamma_g(\theta)}{\cos\theta} = \gamma_0 + (\frac{\epsilon_\infty}{a_x} - \frac{G}{ea^*})\frac{\theta}{\theta_0} + \frac{G\pi^2}{6ea^*}\left(\frac{\theta^3}{\theta_0^3}\right). \tag{28}$$

Marchenko's full result replaces Eq. (25) by

$$\gamma_g(\theta) = \gamma_0(\theta) - \frac{G}{\pi a^*}\sin(\pi\frac{\theta}{\theta_0}). \tag{29}$$

When expressed as an expansion in θ, up to $O(\theta^3)$, for small θ_0, Eq. (29) becomes identical to Eq. (28), once again confirming that our model is identical to Marchenko's model at $T = 0$. In the following section we derive the finite temperature extension of Eq. (28).

B. Phase Diagram for $T > 0$

At finite temperatures, it becomes favorable to form kinks in the steps for entropic reasons. This causes the steps within a bunch to fluctuate from their mean positions, leading to a decrease in the free energy. On general physical grounds then, we expect the free energy per step in larger bunch sizes to decrease less rapidly compared to smaller bunches as steps within larger bunches will have their fluctuations more constrained. If this happens, the free energies of smaller bunches will fall below those of larger bunches. We then expect larger bunches to rearrange themselves into smaller bunches, with increasing temperature, until eventually at very large temperatures only one step is left in the bunch. In this section, we show that this indeed happens.

In order to compute the bunch size at a given temperature in the EDL, it is not necessary to solve the step problem in the thermodynamic limit, or equivalently the hard core boson for a large number of bosons confined to very large number of sites. Instead, computing the energy per boson in a bunch by solving the bunch problem by exact diagonalization is sufficient. This simplification can be understood by noting that bunch-bunch interactions give rise to corrections to the ground state energy that are smaller than the leading bunch energy by a factor s^2, where s is the boson density introduced earlier. As a result, in the limit that the interaction between the bunches are ignored, comparing the energy per boson in bunches of different sizes will determine the stable bunch size. Even computing the ground state energy of a bunch confined on a large number of lattice sites could be difficult due to demands on computational resources. However, for studying the transitions from bunch of size n_b to $n_b - 1$ ($n_b > 2$), the bunches are sufficiently bound that a small number of lattice sites (typically twice to thrice the bunch size) is sufficient to get accurate answers. We will present more details on this in the discussions to follow.

Following the notation introduced for $T = 0$, we write the energy per boson as

$$\frac{E_0[N, T, n_b]}{N} = \hat{\eta}(T) + f(n_b, T) + O((N/L)^2), \tag{30}$$

where in the EDL, the bunch size n_b is obtained by minimizing $f(n_b, T)$, which is the contribution to the energy arising from interactions within a bunch. It is obtained by solving for the ground state energy of Hamiltonian given in Eq. (11) for n_b bosons. We illustrate the results of this procedure in Fig. (5) for $u/g = 1.65$. Here the energy per boson is plotted as a function of inverse temperature $g = G/t$ for $n_b = 2, 3$ and 4. At low temperatures ($g > 6.8$), the energy per boson in the 3-bunch the lowest value, while at moderate temperatures ($6.8 > g > 4.54$) the 2-bunch gives lowest energy per boson, while at high temperatures ($g < 4.54$) the 1-bunch has the lowest energy (the 1-bunch becomes stable when $f(2, T) = 0$). From our results we have computed phase boundaries, shown as the solid curves in Fig. (6), for transitions from 1-bunch to 2-bunch, from 2-bunch to 3-bunch, and from 3-bunch to 4-bunch. In order to obtain the phase boundaries between the n_b-bunch phase and the $n_b - 1$ phase for a fixed u/g, one has to find the value of g that satisfies the equation $f(n_b, T) - f(n_b - 1, T) = 0$. We do this numerically by using a standard root finding algorithm which approaches the root iteratively [19]. The root finding algorithm requires repeated evaluation of $f(n_b, T) - f(n_b - 1, T)$ using exact diagonalization of the n_b and $n_b - 1$ bunches for different values of g.

A key feature of plots shown in Fig. (5) is that the energy curves for bunches that differ in size by one intersect with a finite slope. This means that the derivative of the free energy of the vicinal surface with respect to temperature, or the entropy, is discontinuous at the transition, implying that the the transitions are first order in the EDL. In the next section we will argue that, when bunch-bunch interactions are taken into account, the discontinuity in slope can vanish and the transition becomes continuous.

In calculating the energy of the 3-bunch and 4-bunch, we confined the bosons to 12 sites on a ring, while for the 2-bunch, 200 sites.The latter is equivalent to a 1-body problem describing the relative motion. These ring sizes are sufficient to get accurate answers because the bunches are tightly bound with a mean particle spacing between 1 and 1.5, so that as long as the ring is bigger than about twice the bunch size, the energies do not change much. We have also computed the ground state energies using the GFMC method for bunches confined on lattices with up to 100 sites and verified that the energies plotted in Fig. (5) are accurate. In Fig. (7) we show the energies computed for a 3-bunch on 12 sites using exact diagonalization and on 30 and 100 sites using GFMC(see Sec. VI for details on GFMC simulations). For sake of completeness, we have computed the mean particle spacing for the 3-bunch along the phase boundary separating the 2-bunch and 3-bunch regions and for the 4-bunch along the phase boundary marked between the 3-bunch and 4-bunch regions (see Fig. (6)). These spacings vary from about 1.3 to 1.6 lattice spacings as u/g is varied from its values at the transition onsets up to $u/g = 3$. It is clear that the bunches are very tightly bound in all the cases.

It is of considerable interest to understand how the limit $g \to 0$ is approached for our model. This limit, where only a near-neighbor interaction remains, has an exact solution (see, *e.g.* Refs. [9,20]) involving a first-order phase transition from a gas (infinitely dilute) of 1-bunches to a condensed phase (an ∞-bunch). Note from Fig. (6) that the 2-3 boundary crosses the 1-2 boundary at $u/g = 2.4$ so that a 2-bunch is no longer stable for $u/g > 2.4$. We also show the 1-3 transition line extending from $u/g = 2$ upwards. This line cannot be distinguished from the 2-3 line for $u/g > 2.4$, but in fact lies slightly below it and above the 1-2 line. Thus, for $u/g > 2.4$ in Fig. (6) the 1-bunch goes directly to the 3-bunch and then subsequently to the 4-bunch as the temperature or $1/g$ is lowered at fixed u/g. Further computation for values of u/g up to 8, depicted in Fig. (8), reveals that the 3-4 line comes very close to the 1-3 line while remaining below it. We then conjecture that as $g \to 0$ the n-1 transition lines become asymptotically equal for arbitrarily large n. This is clearly an approach to the 1-∞ transition, which is the first-order transition in the pure short-ranged potential case. As the transition in the short-ranged case is at $u = 2$ [9,20], the asymptotic slope of the transition lines should be at $(1/g)/(u/g) = 1/2$. This is indeed the case as seen in Fig. (8).

IV. PHASE DIAGRAM IN THE DILUTE LIMIT

We will now consider the effect of the bunch-bunch interactions that were ignored in the previous section. We adopt the following steps in discussing this effect: (1) Using the general principles of quantum mechanics, we argue that when the the inter-bunch interactions are turned on, the first order transition should become continuous. (2) We then estimate the regions around the first order transition lines (obtained in the previous section) where the inter-bunch interactions become important. (3) Finally, we develop a perturbative approach to compute the free energy to $O(N/L)^3$ in the region where the inter-bunch interactions are small. In the next section, we will then present the results of GFMC simulations on larger systems and show them to be consistent with our simple theory. In particular we compute the 2-point correlation function, which clearly shows the bunching transitions in large systems.

The effects of interactions on the bunches can be understood qualitatively using arguments based on general principles of quantum mechanics. We confine our discussion to those regions in the phase diagram where the n_b-$n_b - 1$ phase boundary is well separated from all the other phase boundaries. Consider Fig. (9), where we schematically plot the energy per step in bunches of size n_b and $n_b - 1$ as a function of the inverse effective temperature g for some fixed value of u/g. This is similar to Fig. (5), which was used to study phase transitions in the extreme dilute limit. In this figure, we identify three regimes, namely, (1) regions where the energy per boson in the n_b-bunch is much lower than the $n_b - 1$-bunch, (2) regions where the energy per boson in both the n_b-bunch and the $n_b - 1$-bunch have comparable values and (3) the regions where the energy of the $n_b - 1$-bunch is much lower than the n_b bunch. In regions (1) and (3) the ground state energy of a system with large number of bosons can be estimated using perturbative methods. Here to leading order the energy of the system is the energy of a bunch times the total number of bunches. The next to leading order comes from the bunch-bunch interactions via an inverse square interaction. In region (2), called the "critical region", the physics is more complicated, since the system has the nearly same energy in both the n_b and $n_b - 1$ bunch phases. In this case we expect a splitting of the energy levels as sketched in Fig. (9), where the degeneracy of the energy levels is shown to be lifted due to bunch-bunch interactions. The extent of the region with significant splitting is denoted by $\Delta g(n_b \to n_b - 1)$. This width, which vanishes in the limit of vanishing densities, can be written as

$$\Delta g(n_b \to n_b - 1) \sim \Delta T_c(n_b \to n_b - 1) \sim s^{p_{n_b}}, \tag{31}$$

where $\Delta T_c(n_b \to n_b - 1)$ is the width, in temperature, of the critical region and the exponent $p_{n_b} > 0$ will be computed later in this section by comparing the free energies of the bunches of size n_b and $n_b - 1$, derived perturbatively. The physics in the critical region is of general interest, and its relevance goes well beyond the problem we are studying. It involves coupling of modes with very different length scales. A tightly bound n_b-bunch in region (3) can be thought of as having phonon excitations involving all the bunches as well as excitations within the bunch. While the wavelength of the former type of excitations is large (of the order of bunch spacing s^{-1}), the latter modes are localized in regions of the order of few lattice spacings. A bunch of size $n_b - 1$ in region (1) will also possess similar excitations on both large and small scales. While the couplings between the excitations on different scales are small in regions (1) and (3), we expect strong coupling between the short and long wavelength modes in the critical region.

A. Perturbative Treatment for Stable Bunches

In order to compute the bunch-bunch interaction energy in regions with stable bunch sizes (like regions (1) and (3) in Fig. (9)), we make the following assumptions: (1) If a bunch has n_b steps, then the stiffness of a bunch is $\Sigma_b = n_b\Sigma$, where Σ is the single bunch stiffness in the continuum limit. (In the discrete model, the kink energy required to make a kink in the bunch becomes $n_b\Gamma$. However, taking the appropriate limit of vanishing a_y would guarantee that the combination $\exp(-\beta n_b\Gamma)/a_y$ would scale like n_b). In making this approximation, we have ignored the contribution to the bunch stiffness that arises from interactions of the steps in the bunch. This is justified by the fact that average spacing in a bunch, for $u/g < 3$, remains well under two lattice spacings,so that the steps in a bunch remain tightly bound as a single entity. The approximation will be less accurate if the step spacing in the bunch is large, in which case bending of steps would also alter the interaction energy within the bunch. (2) The bunches interact with each other with a renormalized inverse square potential of strength $g_b = n_b^3 g$. This approximation is justified by noting that, in the dilute limit, the spacing between the bunches is very large, so that one bunch sees other bunches as if they were single lines without any internal structure. We note that the contributions to the energy of the system arising from the short range bunch-bunch interactions are smaller than the inverse square contribution by a factor proportional to the density of steps $s \ll 1$. This can be shown very easily using a Hartree-Fock estimation of the short-ranged contribution [21]. The energy of the system can then be computed using the Calagero-Sutherland model of hard-core bosons interacting via an inverse square law, for which an exact solution was provided by Sutherland [22]. Using his solution, we can write the energy per site in a system with bunches of size n_b as

$$\frac{E_0[s,T,n_b]}{L} = \frac{[\eta(T) + f(n_b,T)]\,a_x}{a_z} s + \left(\frac{\pi^2 (k_B T)^2 \lambda_b^2 a_x}{6 {n_b}^4 a_z^3 \Sigma}\right) s^3 + O(s^4), \tag{32}$$

where

$$\lambda_b = \frac{1}{2}\left[1 + \sqrt{1 + 2n_b^3 g}\right]. \tag{33}$$

Using the above form of energy, one can compute such quantities as surface stiffness, crystal shapes etc, which we will turn to following a discussion of the physics in the critical region. An important point to make at this juncture is that in the limit of zero temperature, for large n_b, Eq. (32) is identical to Marchenko's result given in Eq. (28). It is then clear that Eq. (32) is the finite temperature extension of Marchenko's result.

B. Analysis of the Critical Region

In the critical region, since the energies of both the n_b and $n_b - 1$ bunches are nearly equal, we retain the terms of order s^3 arising from bunch-bunch interactions. In order to estimate the width of the critical region, we use the criterion $E(s,T,n_b - 1) \approx E(s,T,n_b)$, to obtain

$$s^2 \sim |f(n_b,T) - f(n_b - 1,T)|. \tag{34}$$

If

$$|f(n_b,T) - f(n_b - 1,T)| \sim |\Delta g(n_b \to n_b - 1)|^{\alpha_{n_b}}, \tag{35}$$

we obtain the result $p_{n_b} = 2/\alpha_{n_b}$, for p_{n_b} introduced in Eq. (31). For all the transitions from the 4 to 3 bunches as well as for the transitions from the 3 to 2 bunches we see that the curves for the energy per step intersect with a finite slope for the parameter range that we have studied. This means that for these first order transitions $\alpha_4 = \alpha_3 = 1$, the width of the critical region scales like

$$\Delta T_c \propto s^2. \tag{36}$$

For the unbinding of the 2-bunch to the 1-bunch, we find, for $g < 3/2$, $\alpha_2 = 2/\sqrt{1+2g}$, while for $g > 3/2$, $\alpha_2 = 1$, from which one can infer that

$$\begin{aligned} \Delta T_c(2 \to 1) &\propto s^{\sqrt{1+2g}}, \quad g < 3/2 \\ &\propto \quad s^2, \qquad g \geq 3/2. \end{aligned} \tag{37}$$

As noted earlier the 3 bunch to 1 bunch transition preempts the 2-bunch to 1-bunch transition for $g < 1.86$. The 3 bunch to 1 bunch transition was seen to be first order in the entire range investigated.

Note next that the simplest conjecture for the shift of the transition temperature due to interactions is that it is of the same order of magnitude as the level shift given in Eq. (31). Explicitly, for the transitions that are first order in the EDL,

$$|T_c(n_b \to n_b'; s) - T_c(n_b \to n_b'; 0)| \propto s^2. \tag{38}$$

While we find that all the transition in the model are first order in the EDL, it is interesting to compute the shift in transition temperature for the 2 bunch to 1-bunch transition temperature when $g < 3/2$. With our conjecture, and using Eq. (37) for $g < 3/2$, one obtains

$$|T_c(2 \to 1; s) - T_c(2 \to 1; 0)| \propto s^{\sqrt{1+2g}}. \tag{39}$$

Note that for this case our conjecture indeed yields the result derived within continuum theory [5,6] using renormalization group methods.

While we have used simple arguments to predict the width of the critical region and the shift of the transition temperature, a detailed analysis of the nature of unbinding transitions and the form of the free energy require further study of the many body problem involving the thermodynamic limit. One natural way to study this is by the means of computational methods like GFMC or exact diagonalization methods for large systems. In the following section, we discuss the results obtained using GFMC simulations.

V. QUANTUM MONTE CARLO SIMULATIONS

In the preceding section we argued, on the basis of results for the *extreme* dilute limit from exact diagonalization of small systems, that the bosons undergo bunching transitions as strengths of the interaction parameters are varied. In this section, we will perform calculations on larger systems to directly study the dilute limit and attempt to understand the physics in the "thermodynamic limit". In addition to exact ground state energy, we also study pair correlation functions in order to probe the structure of the many-body state, in particular the occurrence of bunching and transitions between different bunch sizes.

The primary method we use is Green's function Monte Carlo (GFMC) [23], a Monte Carlo method to study ground state properties of quantum many-body systems which is exact for bosons. Variational Monte Carlo (VMC) calculations are performed prior to GFMC, in order to optimize our variational wave function, which is used to generate the initial state and also as the importance function in GFMC. In Appendix II, we present a brief self contained treatment of these methods. The algorithm we use follows closely that of Refs [24,25], which we refer the reader to for more details.

The variational many-body wave function used is of the Jastrow form, written as a product of two body correlations, *i.e.,*

$$\psi_T\left(x_1, x_2, ..., x_N\right) = \prod_{(i,j)} f(|x_i - x_j|), \tag{40}$$

where $|x_i - x_j|$ is the mean distance between particle i and particle j. The function $f(r)$, where r is a positive integer, is chosen to be of the form

$$f(r) = a(r-r_0)^2 + d, \quad r \le r_0$$
$$= 1 - \frac{f_2}{r^\alpha} + be^{-br}, \quad r > r_0, \tag{41}$$

Defining $f(1) \equiv f_1$, we choose $f_2 = (\alpha+r_0)r_0^{\alpha-1}(1-d)$, $b = 1+\alpha/r_0$, $b = \alpha f_2 e^{br_0}/(br_0^{\alpha+1})$ and $a = (-d+f_1)/(1-r_0)^2$, thus reducing our variational parameters to four, namely, f_1, r_0, d and α. We note that the parameters are chosen such that $f(r)$ and df/dr at $r = r_0$ are continuous. These parameters have direct physical implication as shown in Fig. (10).

In both the VMC and GFMC, we used 500 walkers (on the average for GFMC) for computing the averages. In the variational calculation, measurements were made after 10,000 metropolis steps. In the GFMC calculations measurements are made after 10,0000 steps during which system relaxes from the initial variational distribution. Measurements were made for a total of 20,0000 steps, and statistical errors were obtained by dividing these into 200 blocks of 1000 steps each and estimating the variance of the block measurements.

We present results for three separate cases, namely, $u/g = 1.25, 1.65, 2.0$. These cases are chosen so that in the limit of $g \to \infty$ the ground states have bunches of size $2, 3$ and 4 bosons, respectively.

First we show in Table I a comparison of GFMC and exact diagonalization results for the energy of a small system of 3 bosons. In the exact diagonalization the bosons are confined on 12 sites in a ring, i.e., with periodic boundary condition. The results are shown together with those from GFMC for the same system. The agreement is exact. This is to be expected, since GFMC yields exact ground state energies. Also shown are the energies computed by GFMC for a ring of size 30 and 100 respectively. We see that they are indistinguishable from the corresponding results for 12 sites, indicating that at 12 sites the finite-size effect is already negligible. This confirms our earlier conclusion that the 3 bosons are tightly bound. In Fig. (7), we again compare GFMC results for 2- and 3-boson systems on 30 sites with our exact diagonalization results, over a wider range of parameter space. The excellent agreement reassures that our GFMC code is well-behaved, and that the small system sizes used in exact diagonalization calculations of the EDL are justified.

In table II, III, and IV we present the variational wave-function and the energies E_{VMC} and E_{GFMC} and compare them with the approximate energy E_{approx} of the rescaled Hamiltonian given by Eq.(11). (For sake of clarity we do not include the first term which is proportional to the number of bosons, since it does not directly affect the physics of bunching transitions.) For N bosons on L sites, E_{approx} is computed from the energy per boson $f(n_b, T)$ computed using exact diagonalization and the approximate interaction energy using

$$E_{approx} = \frac{Nf(n_b,T)}{n_b} + \frac{\pi^2\lambda_b^2 N^2}{3n_b^4 L^3}, \tag{42}$$

where λ_b is given by Eq.(33). In computing E_{approx}, the value of n_b is obtained from the the phase diagram given in Fig. (6). For all the values of u/g, for large g, we see that there is good agreement between the $GFMC$ and approximate energies and fair agreement for small values of g. These results confirm the approximations made in the analysis of bunching and bunch-bunch interactions. As g is decreased, the system is more quantum mechanical and each bunch is less tightly bound, hence E_{approx} becomes worse. Note that the in all cases $E_{GFMC} < E_{approx}$, which is not surprising since we did not consider the role of the short-range attraction between the bunches in evaluating E_{approx}.

We also calculate the pair correlation function which for L even is defined as

$$g(x) = \frac{L}{2N^2} < \sum_{i \neq i'} \delta\left(x - x_i + x_{i'}\right) >, \tag{43}$$

for $1 < x < L/2 - 1$. The distance is halved due to periodic boundary condition. In the expression for $g(x)$, x_i and $x_{i'}$ are the coordinates of the bosons i and i'.

In GFMC the mixed estimate is used to compute the average indicated in Eq. (43). Recall that the mixed estimate [23] for the expectation value of an operator $\mathcal{O}$ is

$$\langle \mathcal{O} \rangle_{mixed} = \frac{\langle \psi_T | \mathcal{O} | \psi_0 >}{< \psi_T | \psi_0 >}, \tag{44}$$

where $|\psi_0\rangle$ is the ground state wave function while $|\psi_T\rangle$ is the trial wave function. While exact for the energy, this estimator yields an approximate ground state expectation value for other operators. If $|\psi_T\rangle$ is good, a simple extrapolation [23] of the mixed estimate with the variational expectation can lead to a further improved result. Our $|\psi_T\rangle$ is relatively poor, giving variational estimates of $g(x)$ which are rather structure-less in long range, so we did not

attempt this extrapolation. However, as we see below, even with this $|\psi_T\rangle$, $g(x)$'s computed from the mixed estimate clearly shows the bunching structure.

For $u/g = 1.25$, Fig. (11) shows the pair correlation function for 10 bosons on 100 sites respectively. We see that for large g ($g = 20$ and $g = 15$), the pair correlation function shows two equal peaks near $x = 20$ and $x = 40$. Taking into account periodic boundary condition, we see that this indicates the presence of 5 2-bunches in the system. Note that the 2-bunch at $g = 15$ is more loosely bound than the 2-bunch when $g = 20$. When $g = 10$ the system is a completely unbound state. The case $g = 12$ is in the intermediate region, where the pair correlation still has a large peak at the nearest neighbor site, but does not show peaks at positions which indicate the presence of a 2-bunch. This value of g corresponds to a value of the potential such that the system is in the critical region of the phase diagram. In this region the 2-bunch ground state continuously unbinds into one with single bunches.

We next consider the case $u/g = 1.65$, where we study the ground state of 12 bosons on 120 sites. Fig. (12) shows that for large g ($g = 15$ and $g = 7.5$) there is clearly a 3-bunch, which starts unbinding at $g = 6$. At $g = 5$ there is a 2-bunch. This starts to unbind around $g = 4$ to a single bunch ground state. It is clear that the cases $g = 6$ and $g = 4$ fall in the critical region, where the unbinding of a 3 to 2-bunch ground state and 2 to 1 bunch ground state takes place, respectively. From Fig. (13), for $g = 2$, it is evident that a 4 bunch first unbinds to a 3 bunch, then to a 2-bunch and finally a 1-bunch.

In Fig. (14), we show points corresponding to Figs. (11)-(13) on the phase diagram derived for the extreme dilute limit (EDL). Since these points are for larger systems in the dilute limit, with multiple bunches present and interacting, the precise phase boundary locations for these systems are expected to differ from those for the EDL. We see that the behavior of the pairing correlation functions is completely consistent with the conjectured phase diagrams.

VI. EQUILIBRIUM CRYSTAL SHAPES

In this section we will discuss the equilibrium shapes of crystals that have step-step interactions with competing components. The crystal shapes consists of both smooth and rough regions. The latter regions consists of step bunches separated from each other by distances depending on the local curvature of the surface. From the discussions on the phases of vicinal surfaces, it is clear that the size of the bunches depend on the temperature of the crystal. If the bunches have size, say n_b, at low temperatures. the size progressively decreases as the temperature is increased. In the temperature regimes where we can apply perturbative treatments to compute the step energies, we will find the crystal shapes for both cylindrical and 3-dimensional crystals.

A. Cylindrical Crystals

We start with the simple case of a cylindrical crystal where the variations in the shape occur in a 2-dimensional plane i.e, the crystal is infinitely long in the third direction. The crystal shape is obtained by using the projected free energy of a surface of orientation θ with respect to the reference surface using Wulff construction. If one tunes the temperatures such that bunches of size n_b become stable, then, the crystal shape will consist of rough regions that have widely separated bunches of size n_b. The projected free energy for such a surface can be expressed using Eq. (32) as

$$f(s) = \gamma_0 + \eta_1|s| + \eta_3|s|^3 + O(|s|^4), \tag{45}$$

where the contribution $O(|s|^4)$ comes from the short-ranged attractive interaction between the bunches. In the above equation, we have introduced quantities $\eta_1 = [\eta(T) + f(n_b, T)]/a_z$ and $\eta_3 = \pi^2(k_BT)^2\lambda_b^2/(6n_b^4\Sigma a_z^3)$. The crystal shape $z(x)$ is given by

$$\lambda z(x) = \tilde{f}(\eta)|_{\eta=-\lambda x}, \tag{46}$$

where $\tilde{f}(\eta) = min_s[f(s) - \eta s]$ is the Legendre transform of $f(s)$ to the conjugate field η, an λ is parameter fixing the overall size of the crystal [15]. The minimization leads to the result

$$\begin{aligned} z(x) &= 0, \quad x < x_0, \\ &= -\frac{2\sqrt{\lambda}}{3\sqrt{3\eta_3}}[x - x_0]^{3/2}, \quad x > x_0, \end{aligned} \tag{47}$$

where $x_0 \equiv \eta_1/\lambda$. Notice that the crystal the rough regions joins the flat region in a "continuous" with the well known "3/2" exponent. The above expression for crystal shapes holds in regions were there is a bunch of a stable size, so

that free energy of the surface is obtained by perturbative methods. In the critical region, where we do not have an analytical expression of free energy, we will not be able to write down a simple expression like Eq. (47). However, from the general arguments presented in the previous section and the shape of the free energy shown in Fig. (9), we expect the shapes to evolve smoothly as the stable bunch size changes. Finally we note that at very high temperatures, where the stable bunch size becomes one, the free energy reduces to the standard free fermion energy and one recovers the expression for the crystal shape obtained in Ref. [9].

B. 3-Dimensional Crystals

We now turn our attention from the cylindrical crystals to a 3-dimensional crystal. In this case the crystal has flat facets that are joined to the rough regions as shown in Fig. (15). Once again we will focus on temperatures such that the rough regions have stable bunches of size n_b. The orientation-dependent free energy $f(\mathbf{p})$, where $(\partial z/\partial x, \partial z/\partial y) = -|\mathbf{p}|(cos\phi, sin\phi)$, now takes the form

$$f(|\mathbf{p}|) = \gamma_0 + \eta_1(\phi)|\mathbf{p}| + \eta_3(\phi)|\mathbf{p}|^3 + O(|\mathbf{p}|^4), \tag{48}$$

where the coefficients η_1 and η_3 are functions of the orientation ϕ. Note that ϕ is the angle between the $y-$axis and the average direction of steps at a given point on the surface. In the limit $|\mathbf{p}| \to 0$, ϕ is the angle between the $y-$axis and the direction of the facet edge. An important quantity that characterizes the three dimensional crystal shape is the jump in gaussian curvature at the point where the flat facet joins the rough region. The Gaussian curvature $K(x, y)$ of the crystal at any general point $\mathbf{x} = (x, y)$ can be written as [26]

$$K(x,y) = \left. \frac{\lambda^2(1+|\mathbf{p}|^2)^{-2}}{det\left[\partial^2 f(|\mathbf{p}|)/\partial p_i \partial p_j\right]} \right|_{\mathbf{p}(-\lambda \mathbf{x})}, \tag{49}$$

from which the Gaussian curvature in at the facet edge ($|\mathbf{p}| \to \mathbf{0}$) can be cast in the form

$$K(\phi) = \frac{\lambda^2}{\left[6\eta_3(\phi)\left(\eta_1(\phi) + \eta_1^{''}(\phi)\right)\right]}. \tag{50}$$

Using the fact that $\eta_1(\phi) + \eta_1^{''}(\phi) = n_b\Sigma(\phi)/a_z$ and $\eta_3(\phi) = \pi^2(k_BT)^2\lambda_b^2(\phi)/(6n_b^4\Sigma(\phi)a_z^3)$, the bunch stiffness, we find that the jump in Gaussian curvature at the facet edge, ΔK, is satisfies the relation

$$\frac{k_BT\sqrt{\Delta K}}{\lambda} = \frac{n_b^{3/2}a_z^2}{\pi\lambda_b(\phi)}. \tag{51}$$

We see that the for ansisotropic crystals, where the elastic interactions between the steps depend on their orientation, the jump in Gaussian curvature depends on the angle ϕ. In the limit of high temperatures when $\lambda_b \to 1$ and $n_b = 1$, we recover the universal relation first derived by Akutsu *et al* [26]. In the case when $U = 0$, so that $n_b = 1$, Eq. (51) generalizes the expressions that Saam [27] obtained for certain specific values of g, namely, $g = 0, -1/2$ and 2. Note that the jump in curvature in addition to being non-universal depends not only on the strength of the long range interaction, but also on the strength of the short-range attraction through n_b. We note that in temperature window around which the bunch size decreases, we expect the formula derived for the n_b bunch to evolve to the corresponding expression for the the phase with reduced bunch size. However, in the absence of the exact form of free energy in the critical region, we cannot study the details of this evolution.

VII. COMPARISON OF OUR THEORY WITH CONTINUUM THEORIES

Recently the effect of competing short range and long range interactions on the finite temperature phase transitions on vicinal surfaces was considered by Lassig [5] and Bhattacharjee [6]. They studied a continuum version of the model considered in this paper, where the fermions interact via a short range attractive part $-u$ of a range a and an inverse square repulsive long range interaction of strength g. In the continuum theory, all lengths are measured in units of a, which can set to unity without loss of generality. They analyzed the phase transition using renormalization group(RG) techniques. For N fermions on ring of size L, such that $s \equiv N/L \to 0$, they find that for a given g, when the short range attraction is sufficiently attractive, the fermions tend to phase separate. That is, for $u > \frac{\sqrt{1+2g}}{2}$ [30], the fermions on the ring condense into a narrow region. With increasing u, the region's fermionic wave function

becomes more and more localized, or in other words the steps try to form a *single* bunch of macroscopic size N. This picture is fundamentally different from our theory. In our picture, the steps do not phase separate to form a single macroscopic bunch. Instead, they form bunches of a finite size. The bunches then fill the space and interact with each other with renormalized interaction parameters as discussed in the text. With increasing temperature the steps undergo a series of "peeling" transitions where the bunch size progressively decreases by one. As mentioned earlier, the size of a bunch and peeling transitions are lattice effects which are not present in the continuum model. In the continuum model, steps (bosons) are treated as point objects. An infinite number of these points can thus collapse to a space of arbitrarily small size in order to maximize the short-range attraction. Therefore, for the physical region we are concerned with, namely when the range of the short-range attraction is comparable to the "size" of the bosons, the continuum model is not valid. Due to the underlying crystal structure, such a region may well be more relevant for describing the experimental situation of surfaces.

For a fixed strength of the interaction, the continuum theory only captures the onset of the first bunching instability as the temperature is decreased. In our model, the first bunching instability that is encountered on cooling from the high temperature phase is the point where 2-bunches first appear. For this transition, we find quantitative agreement with the continuum RG theory. In particular, the width of the critical region scales with density like $\Delta T_c \sim s^{\sqrt{1+2g}}$ [5] for $g < 3/2$, which is precisely the relation that we obtain in Eq. (39). For $g > 3/2$, the continuum theory fails to make any predictions because of a singularity in the fermionic wave functions. However the natural cutoff present in the lattice model, prevents such a problem in the lattice model.

Our theory of step unbinding and the continuum theory also give very different results for the crystal shapes, as illustrated in Fig. (16). Since the steps phase separate in the continuum theory, there is a slope discontinuity at the place where the facet of the crystal joins the rough part at low temperatures. This discontinuity in slope decreases continuously and vanishes at the tricritical point. Above the tricritical temperature, the rough part joins the facet with the 3/2 exponent. In our model the rough part joins the facet with the 3/2 exponent at all temperatures. As described earlier, the sizes of the step bunches in the rough regions decrease with increasing temperature.

VIII. COMPARISON OF THEORY WITH EXPERIMENTS ON SILICON SURFACES

As noted in the introduction, one of the objectives of the this work is to provide an explanation for the experimentally observed exponents and for the physics of bunching phenomenona. In principle, to accomplish this one would have to carry out the calculations detailed in the text using interaction potentials between steps derived from electronic structure or other quantum mechanical calculations. Since such calculations are not available at this time, we use the simple model with an attractive interaction restricted to only near neighbor sites to explain the experimental observations.

A. Experiments of Song et.al

We first consider the experiments of Song et.al [1–3], where x-ray scattering studies were conducted on Si(113) miscut from the [113] direction towards [001]. It was seen that depending on the slope of miscut surface s, above a temperature $T_c(s)$, the surface is uniformly stepped, while the surface consists of bunched steps below $T_c(s)$. The number of steps in a bunch was seen to be about 22. From the measurements it was inferred that $s \sim |T_c(0) - T_c(s)|^\beta$, with $\beta = 0.42 \pm .1$. Earlier work based on simple mean-field theory [9], predicted this exponent to be $\beta = 1.0$. Recent renormalization group calculations [5,6] predict that the exponent depends on the ratio of the strengths of the attractive and repulsive interaction strengths. In the region where these calculations are valid, the exponent $\beta \geq 0.5$. The exponent $\beta = 0.5$ corresponds to a special point for 1-D systems interacting via the inverse square potential, a point beyond which the renormalization group methods fail. The continuum theories therefore require a particular value for U/G to obtain agreement with experiments. Within our picture we identify the experimentally observed transition as a 1-bunch to 22-bunch transition. While this transition has not been explicitly studied in this paper, we argue that the features of such a transition can be understood based on results obtained in Sec. IV. First note that like the 1-3 transition that we observe for $u/g > 2.4$, a 1-22 transition can easily be expected in a system with a short ranged potential with a more complex structure. Even in a potential with next to near neighbor interaction i.e. $n_s = 2$ and with $U_2 > 0.25$, at $T = 0$, one directly goes from a one bunch to a 3-bunch bypassing the 2-bunch. For potentials with more complicated features, it is conceivable that one may go directly from a 1-bunch to a phase with many steps in a bunch even at $T = 0$. In these systems, one may easily expect a 1-22 transition, just as we observed a 1-3 transition in a simple model. Furthermore, the arguments presented in Sec. IV. on the shift in transition temperature very well apply to the 1-22 transition provided that the free energy curves $f(22, T)$ and $f(1, T)$ intersect with a finite

slope. If this is the case, we find that the shift in transition temperature goes like s^2 from which it follows that $\beta = 0.5$, in agreement with the experimentally observed exponent. Another key point is that when the bunch interactions are taken into account, we have argued that the transitions that are first order in the EDL become continuous. This means that the the exponent β describes a curve of continuous 1-22 bunch transitions rather than a curve of first order transitions associated with a tricritical point.

From an analysis of the x-ray scattering amplitudes Song et.al [2] were able to extract the temperature dependence of the stiffness of the miscut surfaces. Within our bunching picture the stiffness of a bunched vicinal surface can be expressed as [15] $\tilde{\gamma} = \sqrt{\gamma_{||}\gamma_{\perp}}$, where the stiffness along the direction of the steps can be written as $\gamma_{||} = \Sigma_b/\theta$ while the stiffness in the direction perpendicular to the steps is expressed in terms of the surface energy of the miscut surface $\gamma(\theta)$ as $\gamma_{\perp} = \gamma(\theta) + \gamma''(\theta)$. Using Eq. (32), we can write the scaled surface stiffness, $\hat{\gamma}$ in a stable n_b bunch phase as

$$\hat{\gamma} = \frac{a_z^2\tilde{\gamma}}{\pi k_B T} = \frac{\lambda_b}{n_b^{3/2}}. \tag{52}$$

Using the value of scaled stiffness measured [1] for the 2.1^0 miscut surface, $\hat{\gamma} = 1.5$ at $(T - T_c)/T_c \approx 0.15$ (here T_c is the temperature at which the 22-bunch phase emerges) to represent the stiffness of the $n_b = 1$ phase as the critical region is approached and using Eq. (52), we find $g(T_c) \approx 3/2$. Using this value of g and letting $n_b = 22$, we find the scaled stiffness of the bunched phase at $(T_c - T)/T_c = .15$ to be 1.3. This is closer to the experimentally observed value of 2.2 than the value of 0.87 predicted by earlier mean-field studies [9]. We note that there are some uncertainties in the the experimental results for stiffness in the 22-bunch phase and at low temperatures, which might be the cause of the discrepancy between our results and the experimental observations. In Ref. [2], the authors derive an exponent for the temperature dependence of the stiffness by identifying a spinoidal temperature. Within our picture the transition is continuous and a spinoidal temperature does not exist.

Finally, we note that Song *et al* [3] have studied equilibrating bunches and have sucessfully explained the limiting bunch size in terms of the Marchenko groove picture discussed in Section III.A above.

B. Experiments of Sudoh et. al

We now turn to the recent experiments of Sudoh et.al [4] where the morphology of Si(113) surfaces, miscut towards a low symmetry azimuth which is 33^0 away from the $[\bar{1}10]$ direction to the $[\bar{3}\bar{3}2]$ direction was studied using scanning tunneling microscopy. The authors compared surfaces quenched after annealing at various temperatures in the range 600-1000^0C. Annealing at temperatures above 720^0C resulted in single, double, and triple-height steps, while annealing at a temperatures in the range 690-720^0C the average terrace spacing increased due to presence of double, triple, and quadruple-layer steps. The size of the terraces saturate during annealing, indicating that the surface had reached local thermal equilibrium. STM images at 710^0C show a predominance of double steps. The authors also find that the stiffness of the a step is proportional to its height, with an additional stabilization of double height steps.

Most of the features of the above observations can be understood using the model considered in this paper, in which the attractive interaction is restricted to the nearest neighbor site . We conjecture that the temperature around 720^0C corresponds approximately to $u/g \approx 2.35$ and $1/g \approx 0.5$, where the stable phase is the 2-bunch phase. This point is marked as "Su" in Fig. (6). Note that both the 1-2 line and 2-3 lines are very close to this point, while the 3-4 line is also nearby. This means the free energies of the 1,2 and 3 bunches are very close to each other with the free energy of the 2-bunch being the lowest, explaining its stability. Though the 2-bunch is stable in the EDL, the point Su is very likely to be in the critical region, where the 1 and 3 bunch phases are stabilized by bunch interactions. Further decreasing the temperature results in the emergence of the 4-bunch phase, which can be understood by noting that the system then moves closer to the 3-4 line resulting in the stabilization of the 4-bunch due to bunch interactions. We also point out our arguments that the stiffness of the bunched steps should be proportional to the number of steps in the bunch is also borne out in the experiments. Also, note that this vicinal surface oriented in a direction different from that of Song et.al. As a result we expect different strengths of attractive and repulsive step interactions leading to different bunch sizes in the two experiments.

Step bunches with n_b in the range 1-4 have also been seen on miscut Si(113) by other workers, specifically van Dijken *et al* [28] and Zhu *et al* [29]. Equilibrium does not appear to have been achieved in these cases.

IX. DISCUSSION AND FUTURE DIRECTIONS

In this paper we have explored the phase transitions arising in vicinal surfaces with competing long-range and short range interactions. We showed that depending on the strength of the interactions and the temperature, the steps on the surface rearranged themselves into bunches. Using a tractable model for step interactions, we showed that the bunch size increased with decreasing temperature through a series of bunching transitions. At $T = 0$, we showed that the bunch phases predicted by our model correspond to well known periodic groove structure first predicted by Marchenko. Our theory can then be considered as an extension of the Marchenko theory to finite temperatures, where changes in the size and number of steps in a groove are brought about by the bunching transitions. The implications to experiments and the physics of crystal shapes was pointed out. We found that the exponent relating the dependence of the transition temperature on the miscut angle, β, expected from our theory to be consistent with the experimentally measured exponent and that the observed features of step stiffness was also in agreement with our theory. We now point out some directions for future theoretical and experimental research that can provide more insights on equilibrium bunching on vicinal surfaces.

On the theoretical/computational side, it is very important to have an accurate determination of the step interaction potential. This can be done through quantum calculations or atomistic simulations using reliable empirical interatomic potentials. Once the step interactions are known, the methods developed in this paper can be used to study the step bunching transitions. On the experimental side more data on surfaces with competing interactions can shed light on the role of attractive interactions on equilibrium bunching properties. In particular for vicinal surfaces in a bunched phase, the crystal shape will exhibit a Pokrovsky-Talapov transition as the facet is approached. This is also true within the Marchenko picture. An experimental check of this feature would be valuable. It would also be useful to determine the exponent β for a number of different surfaces that have attractive interactions between steps. In contrast to the recent RG calculations that require a particular ratio of the attractive to repulsive interaction strengths to obtain $\beta = 0.5$, our analysis shows that this value of the exponent is robust, applying to all the bunching transitions that are first order in the EDL.

A detailed study of the step phases as a function of orientation of the silicon surfaces away from the [113] direction would be most useful in order to elucidate the connection between the experiments of Sudoh *et al* and those of Song *et al*. Note that miscuts such as those in the former experiments introduce kinks in steps on the Si(113) surface. For small kink densities, the model parameters G, U, and η should have corrections proportional to the kink density. The phase boundaries in Fig. (6) will then shift linearly with kink density, providing a means of tuning the model parameters. For cases such as that marked by Su in Fig. (6), small changes in the kink density would lead to pronounced effects due to the close proximity of phase boundaries.

The quantum n-bunch, or n-mer, phases discovered in this work are highly interesting in their own right, independent of their realization in crystal surface physics. While we expect these phases to be Luttinger liquids well away from transitions from one bunch phase to another, the picture may change in the crossover region where there is a mixing of the long-wavelength modes associated with phonon-like oscillations of the bunches and the modes internal to the individual bunches. In effect, new many-body phases may emerge in the critical region. A detailed study of the crossover region will shed light on some these new physical phenomenon.

X. ACKNOWLEDGMENTS

VBS would like to thank Sanjay Khare and Avraham Schiller for stimulating discussions. The Quantum Monte Carlo Simulations were performed on the IBM SP2 at the Ohio Supercomputer Center.

APPENDIX A: FREE ENERGY OF AN INCLINED SINGLE STEP IN THE TSK MODEL

In this appendix we derive the free energy of a single step placed on a rectangular lattice with lattice constants (a_x, a_y). The step runs on the average at an angle α with respect to the y-axis (The straight step has $\alpha = 0$.). The slope of the step with respect to the y-axis is then $\hat{s} = \tan\alpha$. If the free energy per unit length of the step as a function of $\hat{s}$ is $\hat{f}(\hat{s})$, then in the expansion for small $\hat{s}$

$$\hat{f}(\hat{s}) = \hat{f}_0 + \frac{1}{2}\Sigma\hat{s}^2 + \cdots, \tag{A1}$$

Σ is the step stiffness. To compute $\hat{f}(\hat{s})$, it is easier to first compute the Legendre-transformed free energy

$$\hat{f}(\hat{\eta}) = \hat{f}(\hat{s}) - \hat{\eta}\hat{s}, \tag{A2}$$

where $\hat{\eta}$ is a field coupling to the slope $\hat{s}$ [15]. We assume that in going from one row to the next, the step can follow only three paths. It can go straight to the next row up with energy ϵ_0, to the left one column and then up one row with total energy $\epsilon_0 + \Gamma - \hat{\eta}$, or to the right one column and then up one row with total energy $\epsilon_0 + \Gamma + \hat{\eta}$. The partition function for the step is readily found, yielding the free energy

$$a_y \hat{f}(\hat{\eta}) = \epsilon_0 - k_B T \ln[1 + e^{-\beta(\Gamma-\eta)} + e^{-\beta(\Gamma+\eta)}] \tag{A3}$$

Combining Eqs.(A1-A3) yields (noting that $e^{-\beta\Gamma} \ll 1$ for this model to apply), we obtain Eq. (13) of the text.

APPENDIX B: QUANTUM MONTE CARLO METHODS

Variational Monte Carlo method: This is the simplest way of performing a quantum Monte Carlo simulation. Here, our aim is to have a trial wave function that has a set of parameters that can be varied. One then optimizes these parameters so as to obtain the lowest possible energy. By means of a Monte Carlo simulation, one can compute the energy of a wave-function as a function of the parameters.

We start with writing the trial state $|\psi_T>$ in terms of the configurations of the one dimensional lattice system

$$|\psi_T> = \sum_R |R>< R|\psi_T>, \tag{B1}$$

where the coefficients $< R|\psi_T >$ depend on the set of variational parameters p_i. Here, $|R>$ is a state in configuration space. For example, for N bosons on L sites a configuration could be a state with bosons on lattice sites $[i_1, i_2..i_N]$ such that $1 \leq i_k \leq L$ for $1 \leq k \leq N$. The expectation value of the energy in the state $|\psi_T>$ can be expressed as

$$\begin{aligned} E_T &= \frac{<\psi_T|\mathcal{H}|\psi_T>}{<\psi_T|\psi_T>} \\ &= \frac{\sum_R E_L(R) <\psi_T|R>< R|\psi_T>}{\sum_R <\psi_T|R>< R|\psi_T>}, \end{aligned} \tag{B2}$$

where the local energy in configuration R is defined as

$$E_L(R) = \frac{<\psi_T|\mathcal{H}|R>}{<\psi_T|R>}. \tag{B3}$$

The sum in Eq. (B2), in general impossible to evaluate analytically, can be evaluated by Monte Carlo. One considers the following expression:

$$E_T = \sum_R E_L(R) p(R), \tag{B4}$$

where one interprets

$$p(R) = \frac{<\psi_T|R>< R|\psi_T>}{\sum_R <\psi_T|R>< R|\psi_T>} \tag{B5}$$

as a probability density function. If one then samples M configurations distributed according to $p(R)$ then the exact expression for E_T can be approximated by

$$E_{VMC} = \frac{\sum'_R E_L(R)}{M}, \tag{B6}$$

where the prime is used to represent sum over the configurations. In the limit of large M, E_{VMC} will converge to E_T. The average E_{VMC}, of course, is subject to statistical fluctuations, and one can easily evaluate the statistical error by $\delta E = \sigma_E/\sqrt{M}$. The variance of the local energy, σ_E, is defined as

$$\sigma_E = \sqrt{< E^2 > - < E >^2}, \tag{B7}$$

where $< E >= E_{VMC}$ and $< E^2 >= \frac{\sum_R' E_L^2(R)}{M}$. It is known [31] that σ_E, which has a lower bound of 0, is a better quantity to optimize than E_{VMC}. We use both quantities as indicators in our search of variational parameters.

For each set of variational parameters, we use the Metropolis algorithm to generate a set of M configurations distributed according to $p(R)$. We start with a configuration of M walkers each of which has N bosons randomly distributed on a lattice of one dimensional ring of size L. Each walker then undergoes a "stochastic walk" according to the following procedure: (1) for each boson we pick a near neighbor site randomly and (2) if the site is occupied the boson is not moved, but if the site is empty the boson is moved with probability q given by

$$q = min\left[1, \frac{\psi_T^2|_{new}}{\psi_T^2|_{old}}\right], \tag{B8}$$

where $\psi_T^2|_{new(old)}$ is $\langle\psi_T|R\rangle\langle R|\psi_T\rangle]$ evaluated at R_{new} and R_{old}. This process is repeated sufficient number of times so that one ends up with a set of walkers distributed according to $p(R)$.

Green's Function Monte Carlo method: This is in principle an exact way to calculate the ground state properties of Bose systems. Its required computer time scales algebraically (as opposed to exponentially in exact diagonalization) with system size, thus allowing exact calculations for large systems. Here, one combines random sampling with a simple method to project out the ground state from an arbitrary initial state.

We start with the operator

$$\mathcal{F} \equiv C - \mathcal{H}, \tag{B9}$$

where the constant C, whose choice we discuss below, is to ensure that all matrix elements $\langle R'|\mathcal{F}|R\rangle$ are non-negative. The basic premise of GFMC is that repeated application of $\mathcal{F}$ on an essentially arbitrary initial state will project out the ground state. That is, if an initial state $|\psi^{(0)}>$ has any overlap with the ground state $|\psi_0\rangle$ of $\mathcal{H}$, the process

$$|\psi^{(n)}>=\mathcal{F}^n|\psi^{(0)}> \tag{B10}$$

will lead to $|\psi_0\rangle$ at large n. GFMC is a method to realize the above process by a Monte Carlo random walk.

In order to improve efficiency of the random walk process, one more mathematical manipulation of Eq. (B10) is necessary. This is done by introducing an operator $\tilde{\mathcal{F}}$ whose matrix elements are related to those of $\mathcal{F}$ by a similarity transformation:

$$\tilde{\mathcal{F}}(R', R) \equiv \langle\psi_T|R'\rangle\langle R'|\mathcal{F}|R\rangle/\langle\psi_T|R\rangle. \tag{B11}$$

The stochastic realization of Eq. (B10) is actually with $\tilde{\mathcal{F}}$ instead of $\mathcal{F}$. While mathematically equivalent, the use of $\tilde{\mathcal{F}}$ can significantly reduce the fluctuation of the Monte Carlo process if $|\psi_T\rangle$ is a reasonable approximation of $|\psi_0\rangle$. This is known as importance sampling [23].

The program is then to start with a set of walkers distributed according to $< \psi_T|R >< R|\psi_T >$. These walkers undergo random walks in R-space. For each walker, denoted by R, taking a step in the random walk means randomly selecting and moving to a new position R' with probability $\tilde{\mathcal{F}}(R', R)/\sum_{R'}\tilde{\mathcal{F}}(R', R)$. Note that, due to the structure of $\mathcal{H}$, there are only $\mathcal{O}(N)$ possible R''s and the corresponding probabilities can be easily computed. Because the overall normalization $\sum_{R'}\tilde{\mathcal{F}}(R', R)$ is not a constant, each walker carries an overall weight which fluctuates, or a branching scheme is introduced to allow the total number of walkers to fluctuate, or both.

The ground state energy is given exactly by the so-called *mixed estimate*

$$\begin{aligned} E_0 &= \frac{< \psi_T|\mathcal{H}|\psi_0 >}{< \psi_T|\psi_0 >} \\ &= \frac{\sum_R E_L(R) < \psi_T|R >< R|\psi_0 >}{\sum_R < \psi_T|R >< R|\psi_0 >}, \end{aligned} \tag{B12}$$

where $E_L(R)$ is defined in Eq. (B3). After a sufficient number of steps, the walkers are distributed according to $< \psi_T|R >< R|\psi_0 >$. E_0 can therefore be computed from such walkers as the (weighted) average of $E_L(R)$ with respect to walker positions R, similar to Eq. (B6). We denote this Monte Carlo estimate of E_0 by E_{GFMC}.

Expectation values of operators other than $\mathcal{H}$ can also be computed from the mixed estimate. However, if the operator does not commute with $\mathcal{H}$, this estimate is *not* exact. As we mention in Section V, this is an important distinction which requires careful analysis of the results. There exist ways to improve upon the mixed estimate and to possibly extract exact estimates of expectation values [23,32], but we will not discuss them here.

Now we describe our choice of C. Since we are dealing with a finite number of hard core bosons on a lattice of finite size, the eigenstates of $\mathcal{H}$ are bounded both from above and below. If E_{max} is the highest eigenvalue of $\mathcal{H}$, we choose C such that $C > E_{max}$. This is easily achieved for the problem at hand. On the lattice we put all bosons next to one another and compute the potential energy arising from the long range interactions alone. For N bosons, we choose C as

$$C = 2N + g \sum_{i=1}^{N-1} \frac{(N-i)}{i^2}. \tag{B13}$$

This clearly satisfies $C > E_{max}$, since hopping and the short range attraction can only lower this energy.

---

[1] S. Song and S. G. J. Mochrie, *Phys. Rev. Lett.* **73**, 995 (1994).
[2] S. Song and S. G. J. Mochrie, *Phys. Rev. B* **51**, 10068 (1995).
[3] S. Song *et al*, *Surf. Sci.* **372**, 37 (1997).
[4] K. Sudoh *et al*, *Phys. Rev. Lett.* **80**, 5152 (1998); preprint (to be published).
[5] M. Lassig, *Phys. Rev. Lett.* **77** 526 (1996).
[6] S. M. Bhattacharjee, *Phys. Rev. Lett.* **76** 4568 (1996).
[7] V. I. Marchenko, *Sov. Phys. JETP* **54**, 605 (1981). Note that a factor of 2 should multiply the second line in the equation at the bottom of the first page of this article.
[8] V. B. Shenoy, Shiwei Zhang and W. F. Saam, *Phys. Rev. Lett.* **81** 3475 (1998).
[9] C. Jayaprakash, C. Rottman, and W. F. Saam, *Phys. Rev. B* **30**, 6549 (1984).
[10] P. G. de Gennes, *J. Chem. Phys.* **48** 2257 (1968); For a general review of fermionic methods, see M. den Nijs, in *Phase Transitions and Critical Phenomenon*, Vol. 12, edited by C. Domb and J. L. Lebowitz (Academic, London, 1989).
[11] For a mapping of reconstructed surfaces to the Hubbard model see L. Balents and M. Kardar, *Phys. Rev. B* **46** 16 031 (1992).
[12] See for *e.g.* C. Duport, P. Nozieres and J. Villain, *Phys. Rev. Lett.* **74** 134 (1995); J. Tersoff *et.al, Phys. Rev. Lett.* **75** 2730 (1995); D. Kandel and J. D. Weeks, *Phys. Rev. Lett.* **74** 3632 (1996); D-J. Liu and J. D. Weeks, (*Cond-Mat*/9803173).
[13] E. Fradkin, *Field Theories Of Condensed Matter Systems*, (Addison-Wesley, Redwood City, California, 1991).
[14] V. I. Marchenko and A. Ya. Parshin, *Sov. Phys. JETP*, **52** 129 (1981).
[15] P. Nozieres, in *Solids Far From Equilibrium*, edited by C. Godreche (Cambridge University Press, Cambridge, 1991).
[16] J. Frohn *et.al, Phys. Rev. Lett.* **67** 3543 (1991).
[17] J. C. Heyraud and J. J. Metois, *J. Cryst. Growth* **50** 571 (1980); *Acta Metall.* **28** 1789 (1980).
[18] For a theoretical discussion of the orgin of attractive step-step interactions see A. C. Redfield and A. Zangwill, *Phys. Rev. B* **46**, 4289 (1992) and references therein.
[19] Details of this method can be found in W. H. Press *et.al., Numerical Recipies* (Cambridge University Press, Cambridge, 1987), page 258.
[20] T. W. Burkhardt and P. Schlottmann, *J. Phys. A* **26** L501 (1993).
[21] See Eqs. (8) and (9) of Ref. [9] for a derivation of this result.
[22] B. Sutherland, *J. Math. Phys.* **12** 246, 251 (1971).
[23] M. H. Kalos, *Phys. Rev.* **128**, 1791 (1962); D. M. Ceperley and M. H. Kalos, in *Monte Carlo Methods in Statistical Physics*, ed. by K. Binder (Springer-Verlag, Heidelberg, 1979).
[24] N. Trivedi, D. M. Ceperley, *Phys. Rev. B* **41** 4552 (1990).
[25] Shiwei Zhang *et.al., Phys. Rev. Lett.* **74** 1500 (1995).
[26] Y. Akutsu, N. Akutsu and T. Yamamoto, *Phys. Rev. Lett.* **61**, 424 (1988); *Phys. Rev. Lett.* **62**, 2637 (1989).
[27] W. F. Saam, *Phys. Rev. Lett.* **62**, 2636 (1989).
[28] S. van Dijken *et al*, *Phys. Rev. B* **55**, 7864 (1997).
[29] Jian-hong Zhu *et al*, *Appl. Phys. Lett.* **73**, 2438 (1998).
[30] The formula given in Ref. [5] differs from this formula by a factor of 2 that multiplies g, because of a factor 1/2 in the normalization of the kinetic energy part of the Hamiltonian.
[31] C. J. Umrigar *et. al.*, *Phys. Rev. Lett.* **60** 1719 (1988).
[32] K. J. Runge, *Phys. Rev. B* **45** 7229 (1992); Shiwei Zhang and M. H. Kalos, *J. Stat. Phys.* **70** 515, 1993.

FIGURE CAPTIONS

FIG. 1. Geometry for the TSK model. The steps between terraces are indicated by bonds on the lattice.They run parallel to the y-axis on an average.

FIG. 2. T=0 phase diagram of the vicinal surface plotted as a function of the ratio of the near neighbor attractive interaction U and repulsive inverse square interaction G. The dots separate regions with stable bunch sizes that differ by one (The bunch sizes are given indicated in the figure).

FIG. 3. Plot of the difference in energy per boson in a n_b bunch and the energy of a 1-bunch. At the points indicated by dots, the bunch size corresponding to the minimum of the energy difference increases by one.

FIG. 4. Periodic Groove structure proposed by Marchenko. The figure shows the repeating groove structure (length L_g), the flat facet (length L_1) and the stepped facet (length L_2). The case $n_b = 3$ is shown here for graphical simplicity. Marchenko's calculation applies only for n_b large.

FIG. 5. Energy/step in bunches of size 2(circle), 3(square) and 4(triangle) for $u/g = 1.65$, plotted as a function of g. The energies are obtained by exact diagolization of the quantum bunch problem on 12 sites in the case of 3 and 4 bunches and 200 sites for the 2 bunch.

FIG. 6. Phase diagram in the extreme dilute limit plotted in the u/g-$1/g$ space. The lines separate regions with stable bunch sizes that differ by one. The stable bunch size in each region is indicated in the figure. The 1-2 line (dotted line) lies above the 1-3 line (short-dashed line) for $u/g < 2.4$, while lies beneath it for $u/g < 2.4$. For $u/g > 2.4$ the 1-3 line lies in between the 1-2 and 2-3 (solid line) lines. This implies that for $u/g > 2.4$, the 1-bunch phase directly undergoes a transition to the 3-bunch phase bypassing the 2-bunch phase. The long-dashed line is the 3-4 line.

FIG. 7. Comparison of the exact diagonalization calculations and GFMC simulations. The circles indicate the energy per step in a 3-bunch confined to 12-sites and for a 2-bunch on 200 sites as found from exact diagonalization, while the triangles and squares represent the results for the 2-bunches and 3-bunches on 30 sites and 100 sites, respectively, as found using GFMC. The error bars on the GFMC energies are shown in the figure. Lines are drawn through the points to guide the eye.

FIG. 8. Plot of the 1-3 line and 3-4 line for $u/g < 8$.

FIG. 9. Schematic plot of the energy per step (solid curves) when the bunch-bunch interactions are taken into consideration. The dotted lines indicate the energy per step in the EDL. In Region 1, the n_b-bunch has lower energy while in Region 3 the $n_b - 1$ bunch is lower in energy. In the critical region, the energy per step smoothly passes from $f(n_b, T)$ to $f(n_b - 1, T)$. The width of the critical region indicated in the figure is estimated in the text.

FIG. 10. Schematic depiction of the two body correlation $f(r)$ used in the trial wave-function. The function $f(r)$ takes on a value f_1 at $r = 1$ has a minimum value of d at $r = r_0$ and behaves like $1 - const/r^\alpha$ for large r.

FIG. 11. The boson pair correlation function $g(x)$ for 10 bosons on 100 sites with $u/g = 1.25$ for values of g indicated in the figure. The points are also marked in Fig. (14) for comparison. By counting the number of peaks in $g(x)$ and making use of the periodic boundary condition the number of bosons in a bunch can be established. For example, in the case $g = 20$, there are 2 peaks at $x = 20$ and $x = 40$ in addition to a large value of $g(x)$ on the near neighbor site. Invoking the periodic boundary condition, one sees that if there are 2 bosons in a bunch, the four peaks at $x = \pm 20$, $x = \pm 40$ account for 8 bosons, which along with the boson on the near neighbor site and the boson at the origin add up to 10 bosons. For $g = 20$ and $g = 15$ we have a well defined 2-bunch phase, while there is a well defined 1-bunch phase for $g = 10$. The figure shows that $g = 12$ is in the critical region. We illustrate the statistical error bars only for the case $g = 20$, since in all the other cases they have similar magnitudes.

FIG. 12. Boson pair correlation function (Eq. (43)) for 12 bosons on 120 sites with $u/g = 1.65$ for values of g indicated in the figure. The points are also marked in Fig. (14) for comparison. Counting the number of peaks as we did in Fig. (11) gives the number of bosons in a bunch. To account for the 3-bunches, note that when $g = 15$ there are 2 peaks at $x = 30$ and $x = 60$ in addition to large values of $g(x)$ on the near-neighbor and next to near-neighbor sites. Invoking the periodic boundary condition, we see that the peaks at $x = \pm 30$ account for 6 bosons while the peak at $x = 60$ accounts for 3 bosons which along with the boson at the origin and the ones on two adjacent sites account for all 12 bosons. For $g = 15$ and $g = 7.5$ we have a well defined 2-bunch phase, while there is a well defined 2-bunch phase for $g = 5$ and 1-bunch phases for $g = 4$ and $g = 3$. The figure shows that $g = 6$ is in the critical region. The statistical error bars for all values of g have about the same magnitude as the case $g = 15$ where they have been explicitly displayed.

FIG. 13. Boson pair correlation function (Eq. (43)) for 12 bosons on 120 sites with $u/g = 2.0$ for values of g indicated in the figure. The points are also marked in Fig. (14) for comparison. By counting the number of peaks in $g(x)$ as we did in the previous figures, we see that for $g = 7.0$, $g = 3.5$, $g = 2.85$ and $g = 2.25$ we have well defined 4,3,2 and 1-bunch phases respectively, while the points $g = 4$ and $g = 2.96$ are in the critical region. The error bars have only been shown for the case $g = 7$, since in all the other cases they have similar magnitudes.

FIG. 14. Comparison of the phase diagrams obtained in the EDL using exact diagonalization and GFMC simulations. For $u/g = 1.25, 1.65, 2.0$ the pair correlation functions for the marked values of g are given in Fig. (11)-(13). For each value of g we also indicate the bunch size (1b,2b,3b and 4b correspond to 1,2,3 and 4 bunches respectively, while cr refers to the critical region) obtained from GFMC simulations. Note that the GFMC results and the exact diagonalization results do not agree exactly since in the dilute limit the bunch interactions can alter the nature of the phases especially close to the phase boundaries.

FIG. 15. Top view of a 3-d crystal. The flat facets and the rough regions are shown in the figure. The steps in the rough region run parallel to the direction inclined to the vertical by an angle ϕ as shown, for a point at the facet edge, in the figure. The z-axis points outside the plane of the paper as indicated in the figure.

FIG. 16. Comparison of the temperature dependence of crystal shapes in lattice and continuum theories. In the lattice theory the rough region always joins the facet continuously with the standard "3/2" exponent. In this theory, the rough regions consists of steps in bunches, whose sizes decrease with increasing temperature. Within the continuum theory, the rough regions joins the facet with a discontinuous slope. This discontinuity decreases with increasing temperature and vanishes at the tricritical point.

TABLES

TABLE I. Comparison of the exact diagonalization and GFMC results for 3 bosons confined on 12 sites with $u/g = 1.65$. E_{exad} denotes the energy per boson obtained by exact diagonalization, E_{var} is the variational energy per boson on 12 sites and E^{12}_{GFMC} represents the GFMC result. The number bracket, corresponding to the GFMC energies, indicates the error on the last decimal place. In all the cases a variational wavefunction with $r_0 = 3$, $f_1 = 1.14$, $d = 0.5$ and $\alpha = 0.6$ was chosen. We also give the GFMC energies ,E^{30}_{GFMC} andE^{100}_{GFMC} , for 3 bosons occupying 30 and 100 sites respectively.

g	E_{exad}	E_{VMC}	E^{12}_{GFMC}	E^{30}_{GFMC}	E^{100}_{GFMC}
6.5	-0.44902	-0.34(3)	-0.4489(2)	-0.4490(4)	-0.4492(7)
6.9	-0.57562	-0.47(3)	-0.5756(1)	-0.5756(4)	-0.5753(6)
7.3	-0.70425	-0.63(4)	-0.7042(1)	-0.7043(4)	-0.7046(6)

TABLE II. Energies for $u/g = 1.25$ and values of g shown in the table, computed for 10 bosons on 100 sites. The variational energy is denoted by E_{VAR}, the GFMC energy by E_{GFMC} and E_{approx} is the approximate energy computed using Eq. (42). The variational wave function parametrized by r_0, f_1, d and α (see Eq. (41)) is also tabulated.

g	r_0	f_1	d	α	E_{VMC}	E_{GFMC}	E_{approx}
10.0	2.0	1.05	0.58	1.5	3.63(4)	2.312(1)	3.071
12.0	2.0	1.06	0.58	1.5	3.76(5)	2.221(1)	3.553
15.0	2.0	1.06	0.30	0.5	2.37(6)	-0.479(1)	-0.424
20.0	2.0	1.14	0.18	0.5	-0.10(1)	-6.701(2)	-6.223

TABLE III. Energies for $u/g = 1.65$ and values of g shown in the table, computed for 12 bosons on 120 sites. The symbols have same meanings as in Table. II

g	r_0	f_1	d	α	E_{VMC}	E_{GFMC}	E_{approx}
3.0	4.0	1.02	0.7	1.0	1.99(2)	1.139(1)	1.311
4.0	4.0	1.02	0.3	0.4	1.85(4)	1.032(1)	1.579
5.0	4.0	1.02	0.4	0.4	0.40(3)	-0.620(1)	-0.486
6.0	4.0	1.14	0.1	0.1	-1.68(9)	-3.340(3)	-3.363
7.5	4.0	1.14	0.1	0.1	-6.83(7)	-8.870(7)	-8.742
15.0	4.0	1.16	0.1	0.1	-33.77(3)	-39.075(3)	-38.814

TABLE IV. Energies for $u/g = 2.0$ and values of g shown in the table, computed for 12 bosons on 120 sites. The symbols have same meanings as in Table. II

g	r_0	f_1	d	α	E_{VMC}	E_{GFMC}	E_{approx}
2.25	3.0	1.04	0.7	0.7	1.11(1)	0.807(1)	1.104
2.85	3.0	1.06	0.5	0.1	0.89(1)	0.051(5)	0.119
2.96	4.0	1.02	0.1	0.1	0.34(2)	-0.301(1)	-0.209
3.5	4.0	1.02	0.1	0.1	-2.31(3)	-3.181(1)	-3.160
4.0	4.0	1.06	0.1	0.1	-4.61(1)	-6.165(5)	-6.144
7.0	4.0	1.06	0.1	0.1	-24.21(3)	-26.779(1)	-26.665

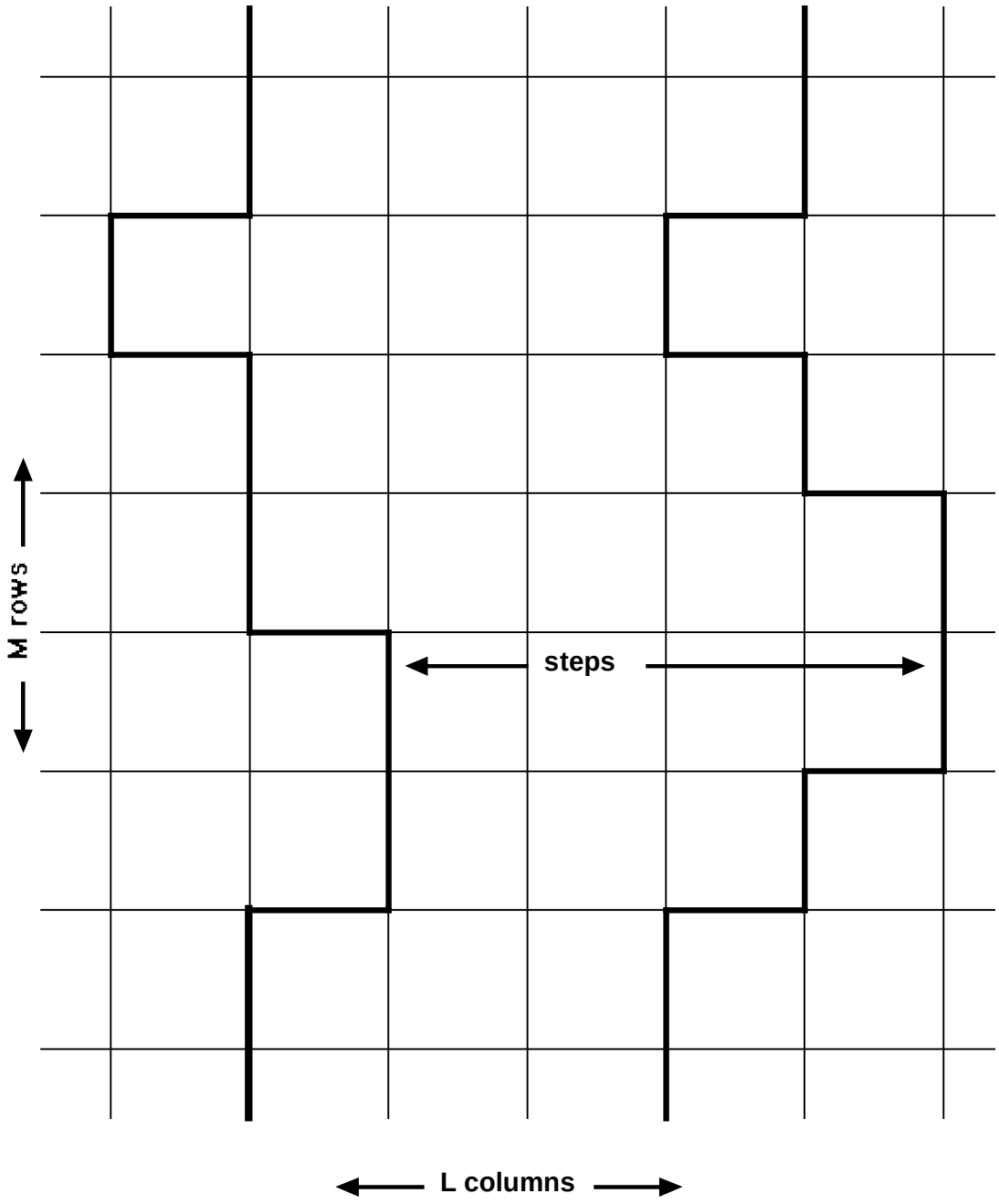
M rows
steps
L columns

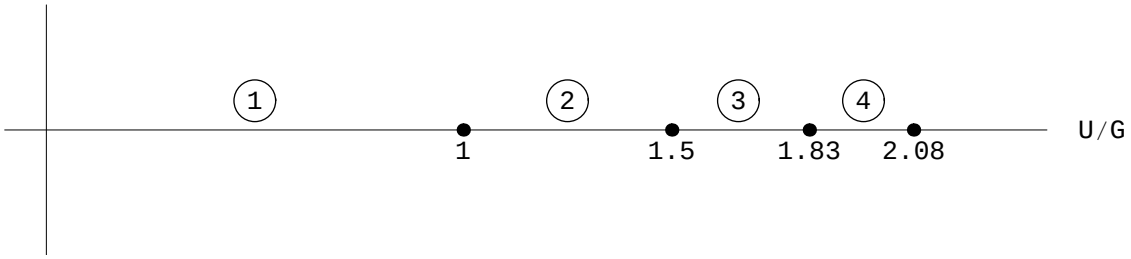
1
2
3
4
1
1.5
1.83
2.08
U/G

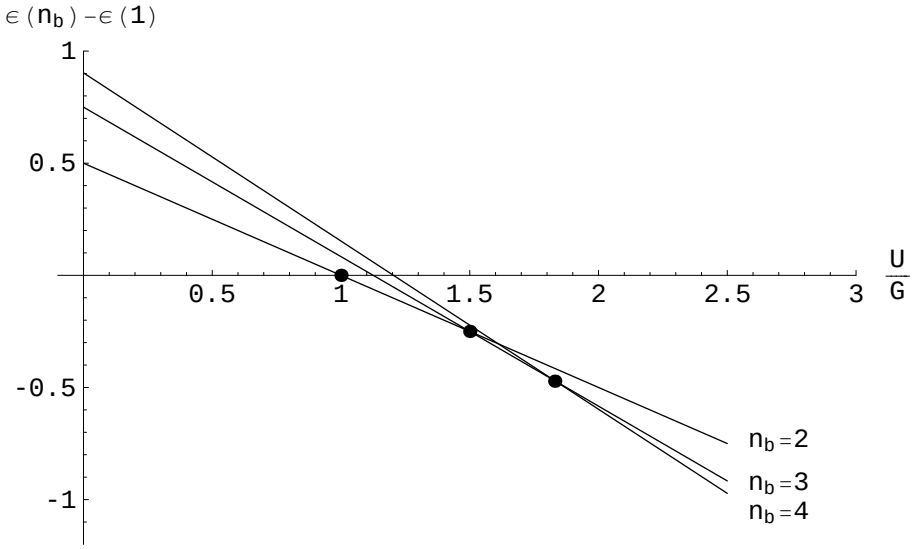
∈(n_b)−∈(1)
1
0.5
-0.5
-1
0.5
1
1.5
2
2.5
3
U/G
n_b=2
n_b=3
n_b=4

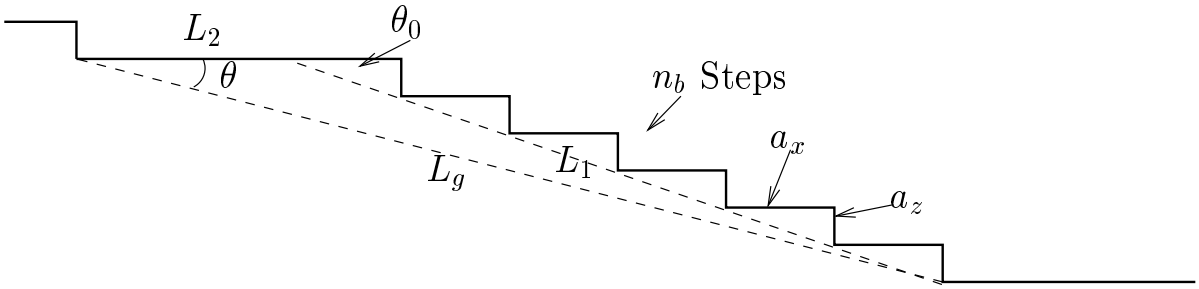
L_2
θ_0
θ
n_b Steps
a_x
L_g
L_1
a_z

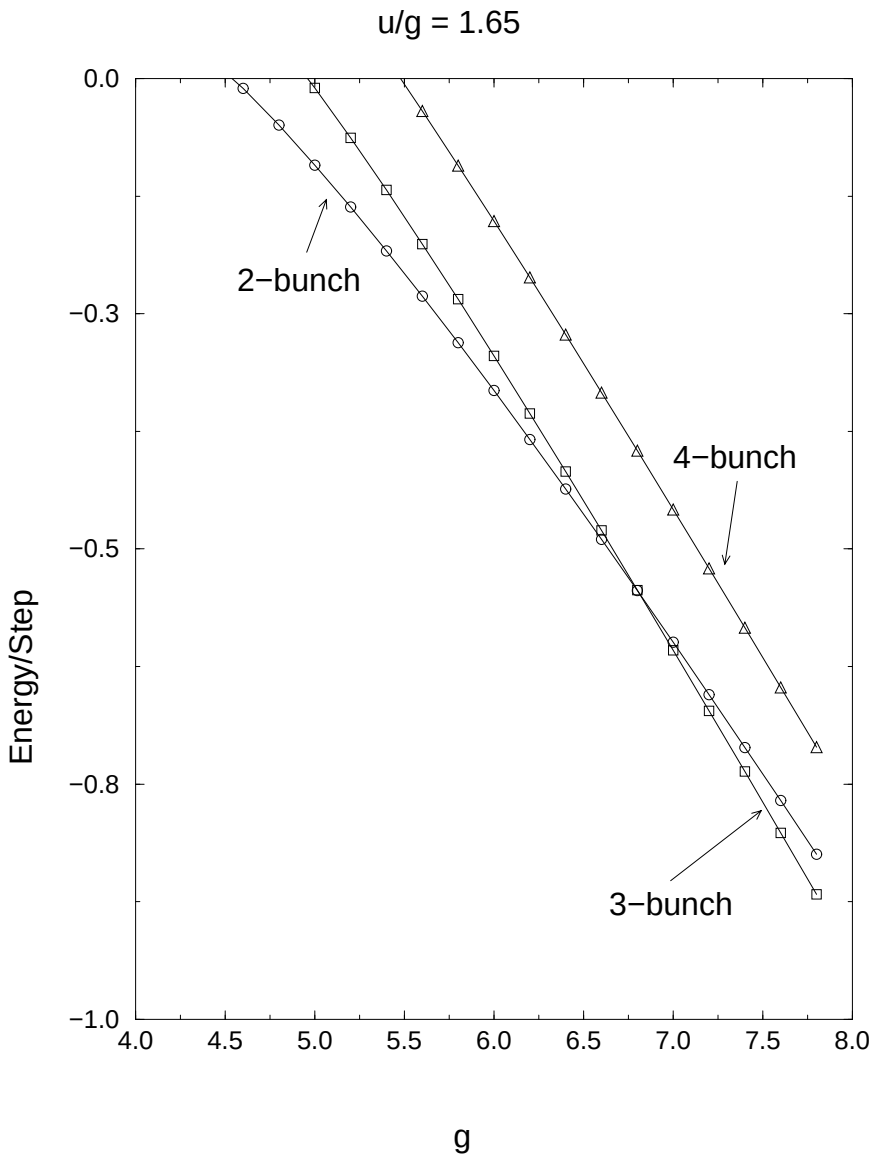
u/g = 1.65
0.0
−0.3
−0.5
−0.8
−1.0
4.0
4.5
5.0
5.5
6.0
6.5
7.0
7.5
8.0
Energy/Step
g
2−bunch
3−bunch
4−bunch

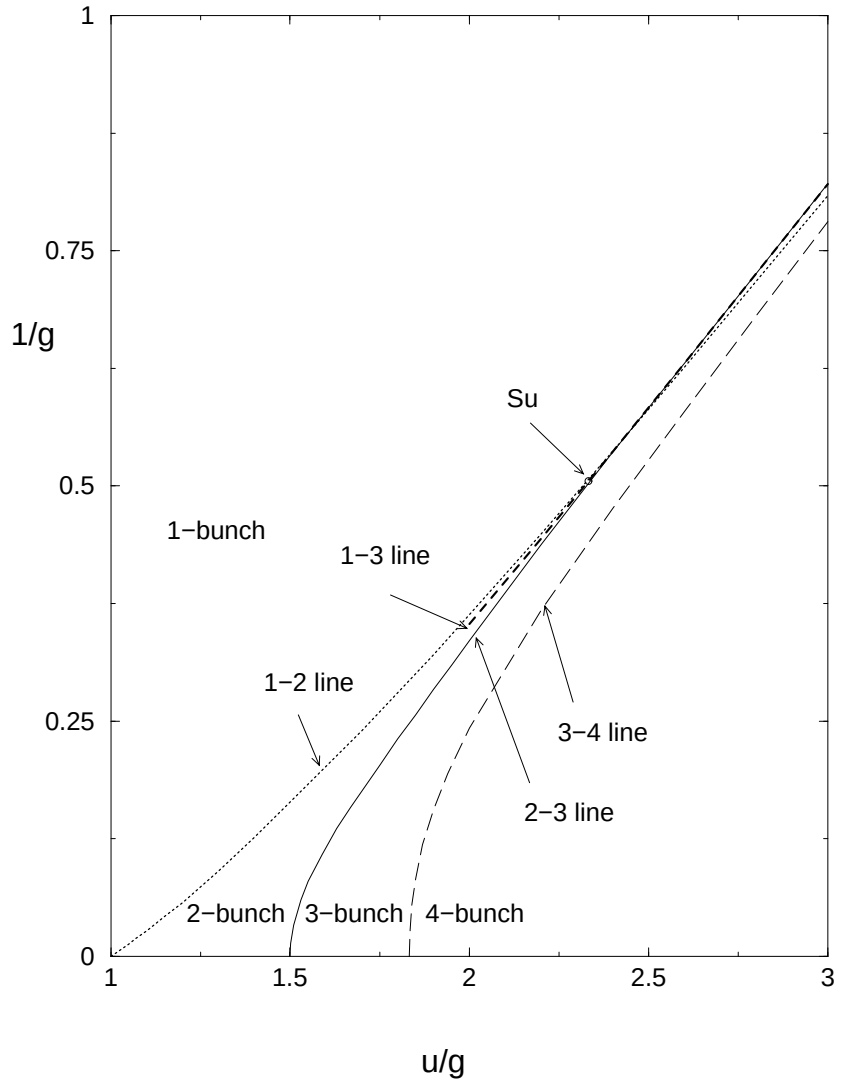
1
0.75
0.5
0.25
0
1/g
1
1.5
2
2.5
3
u/g
Su
1−bunch
1−3 line
1−2 line
3−4 line
2−3 line
2−bunch
3−bunch
4−bunch

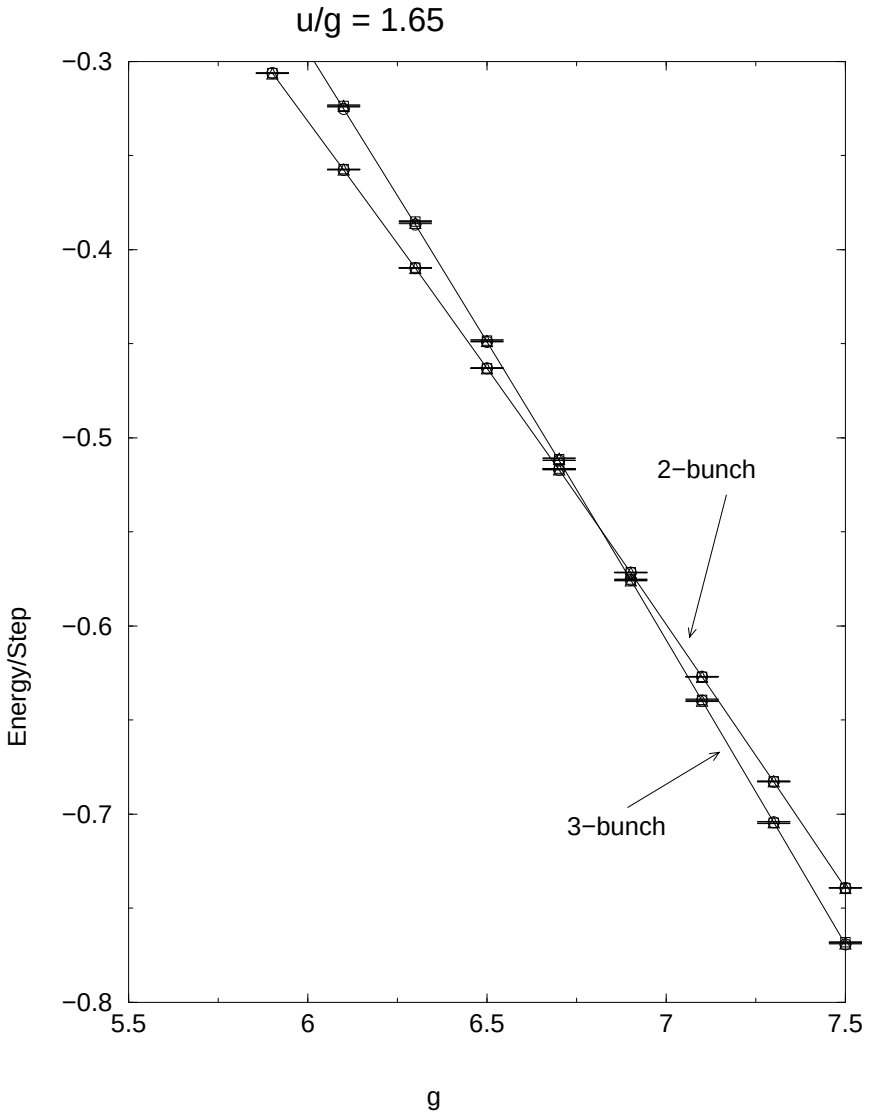
u/g = 1.65
−0.3
−0.4
−0.5
−0.6
−0.7
−0.8
Energy/Step
5.5
6
6.5
7
7.5
g
2−bunch
3−bunch

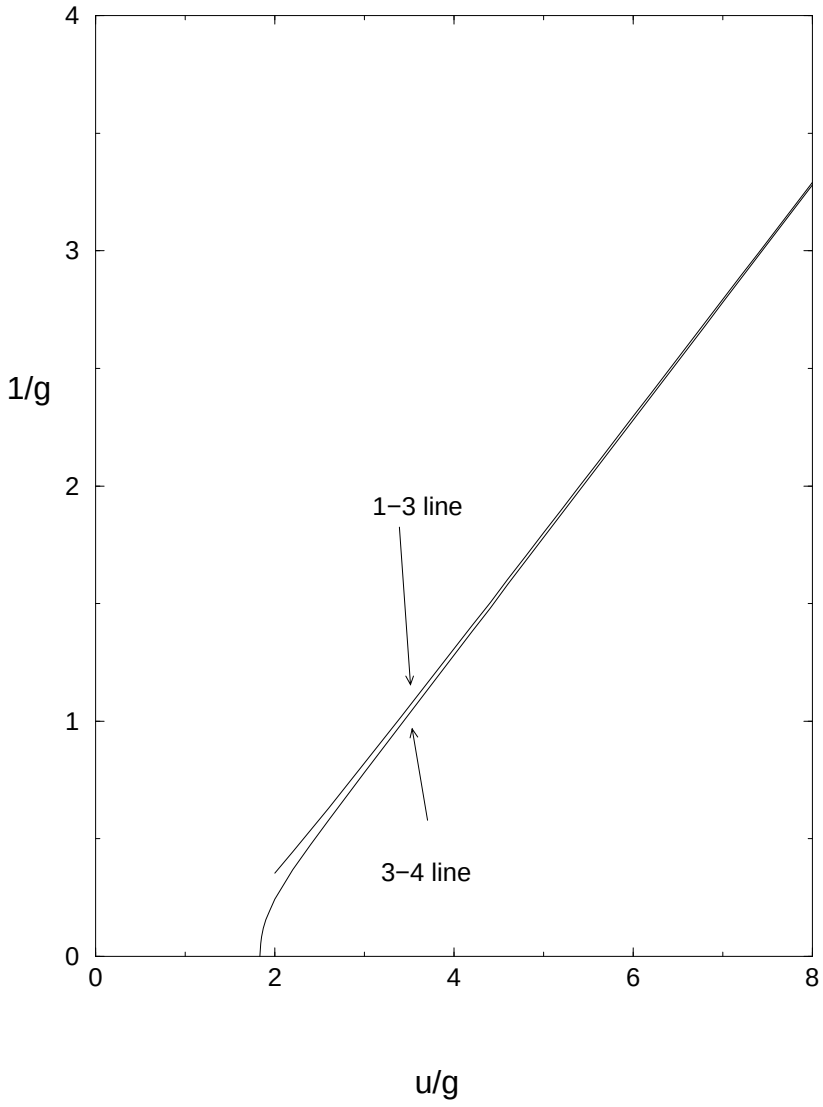
4
3
2
1
0
1/g
0
2
4
6
8
u/g
1−3 line
3−4 line

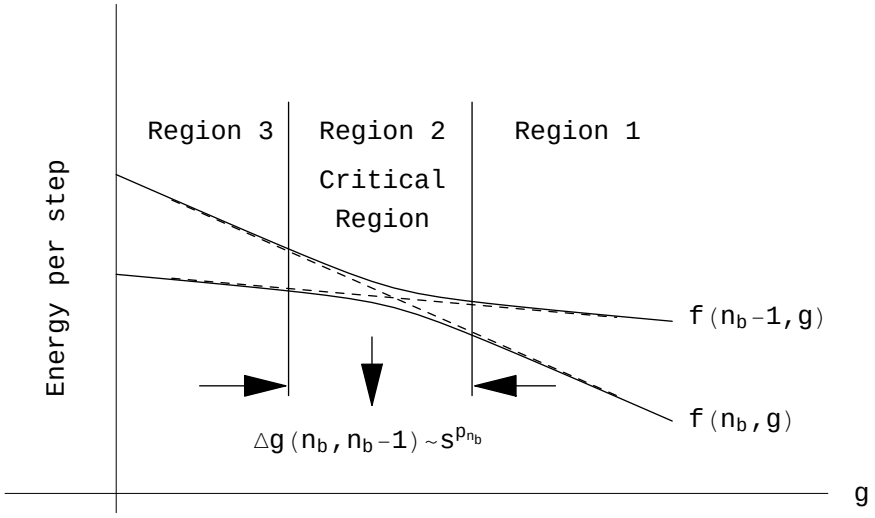
Region 3
Region 2
Critical
Region
Region 1
Energy per step
$f(n_b-1,g)$
$f(n_b,g)$
$\triangle g(n_b,n_b-1)\sim s^{p_{n_b}}$
g

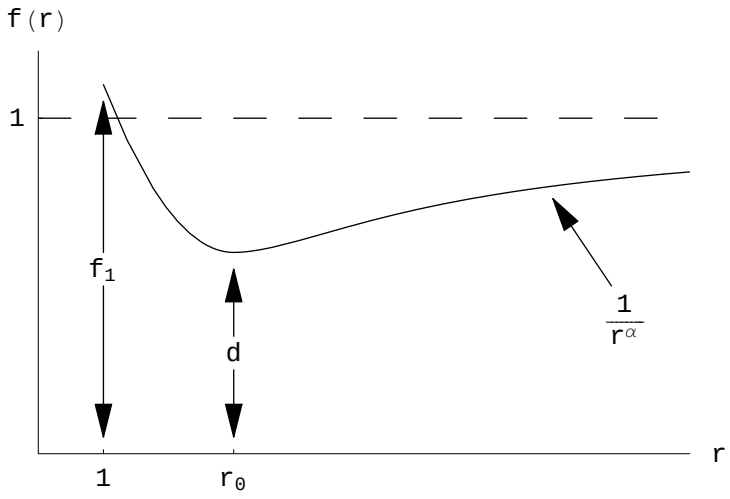
f(r)
1
f_1
d
$\frac{1}{r^\alpha}$
r
1
r_0

u/g=1.25, 10 Bosons on 100 Sites

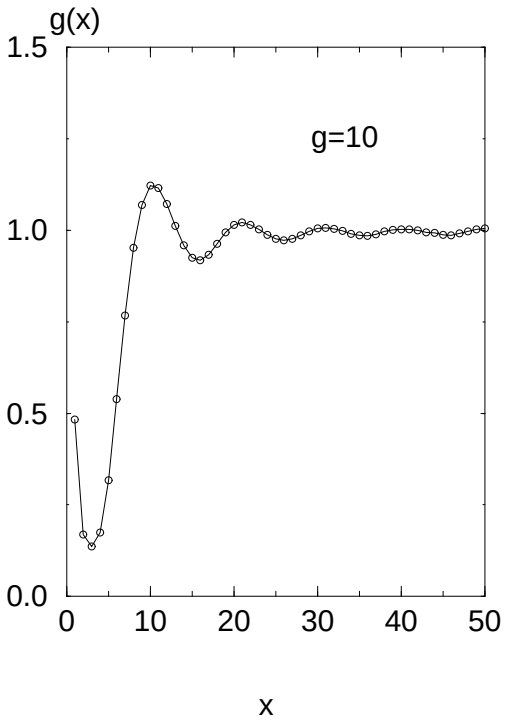

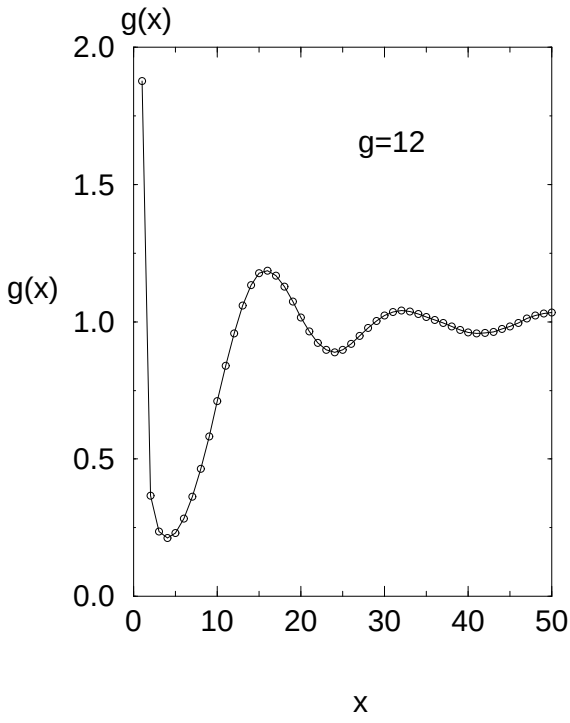

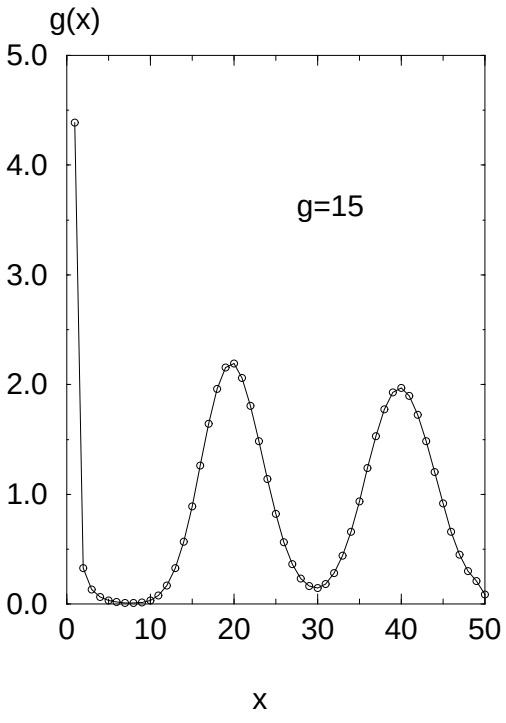

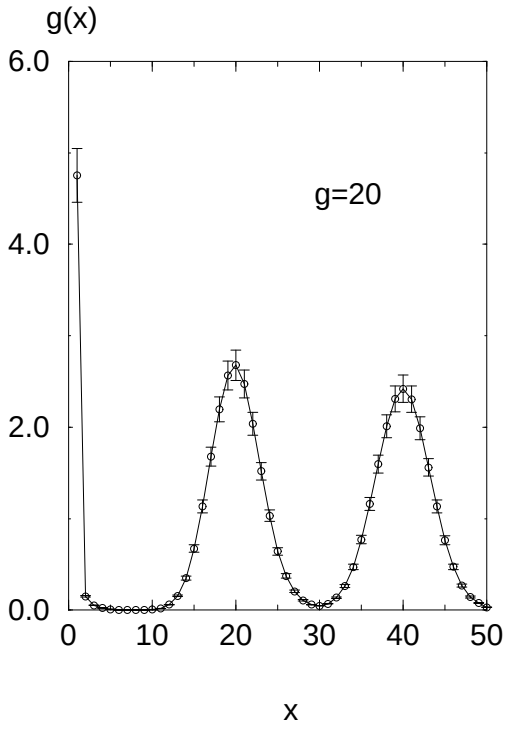

u/g=1.65, 12 Bosons on 120 Sites

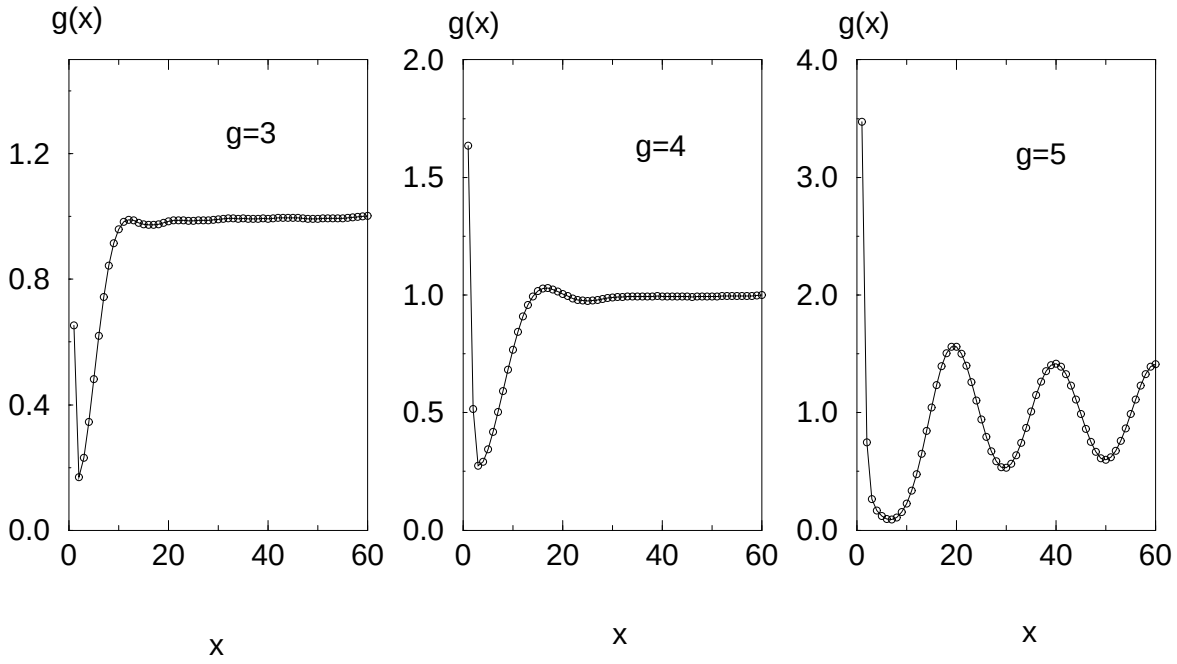

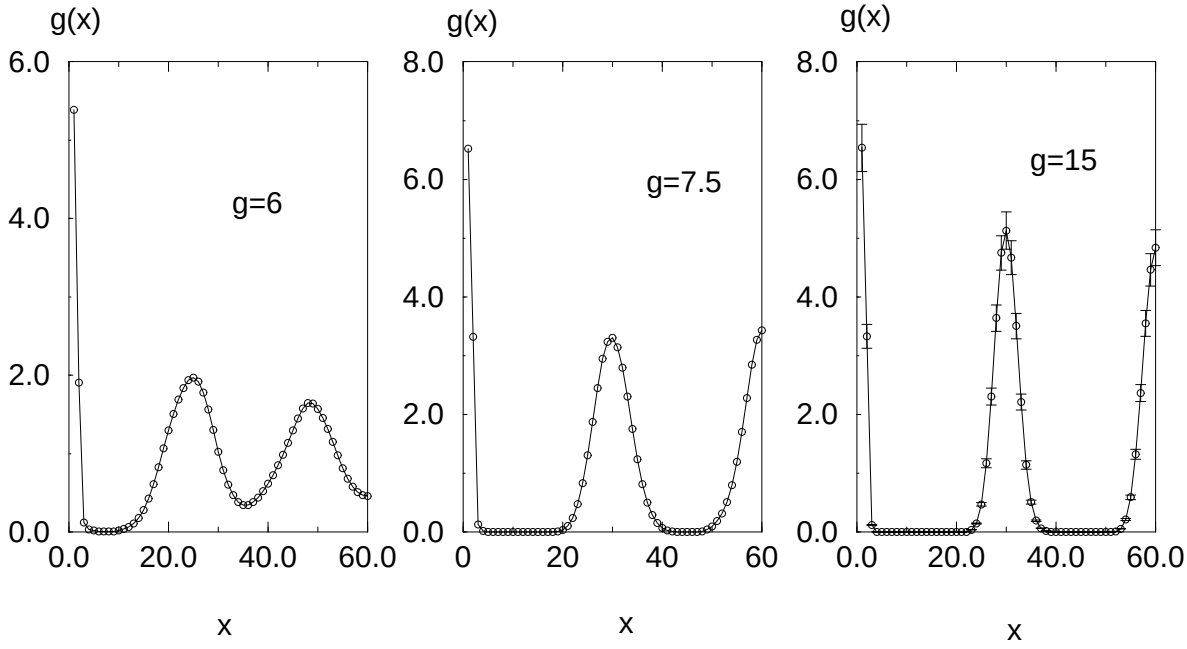

u/g=2, 12 Bosons on 120 Sites

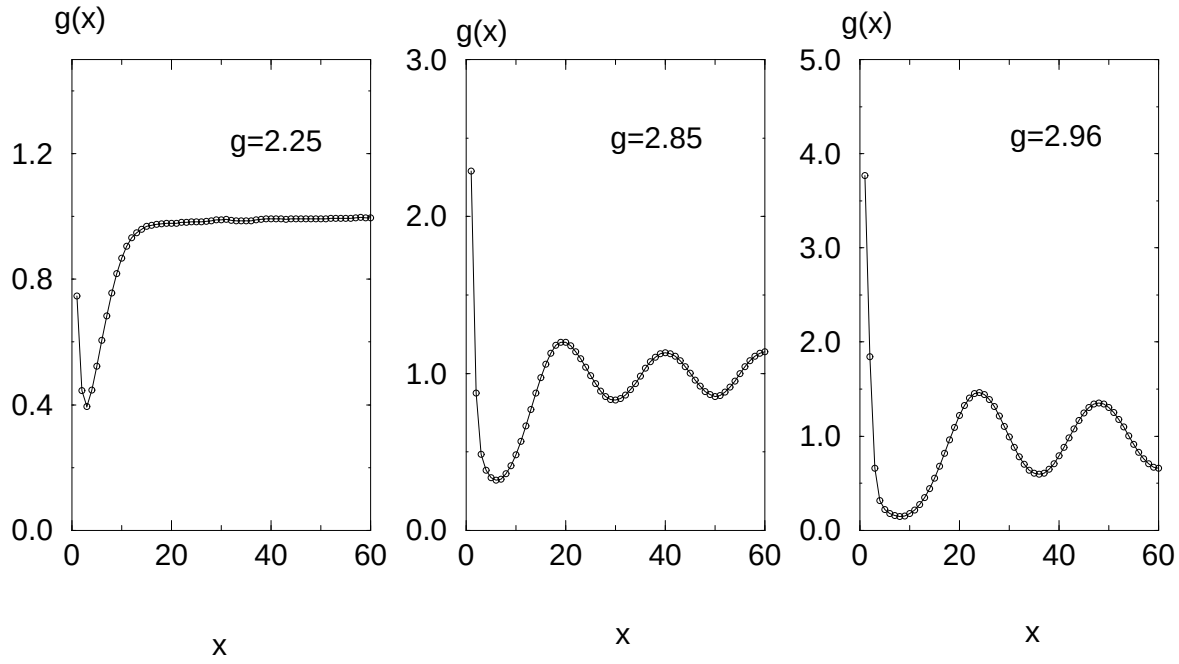

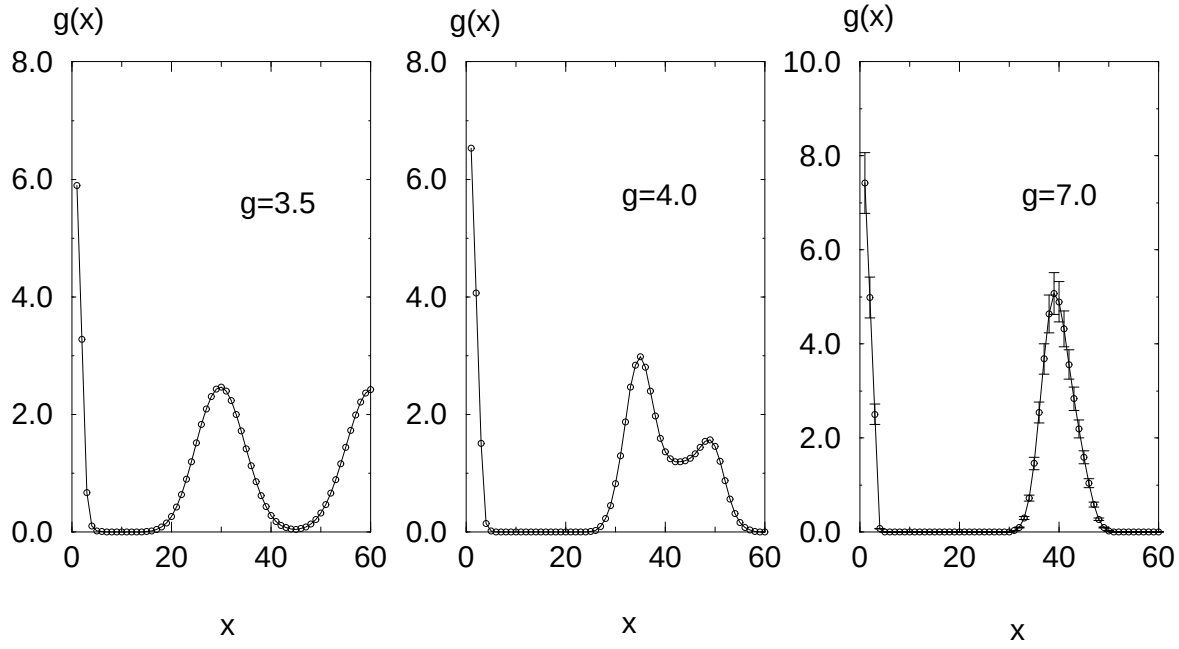

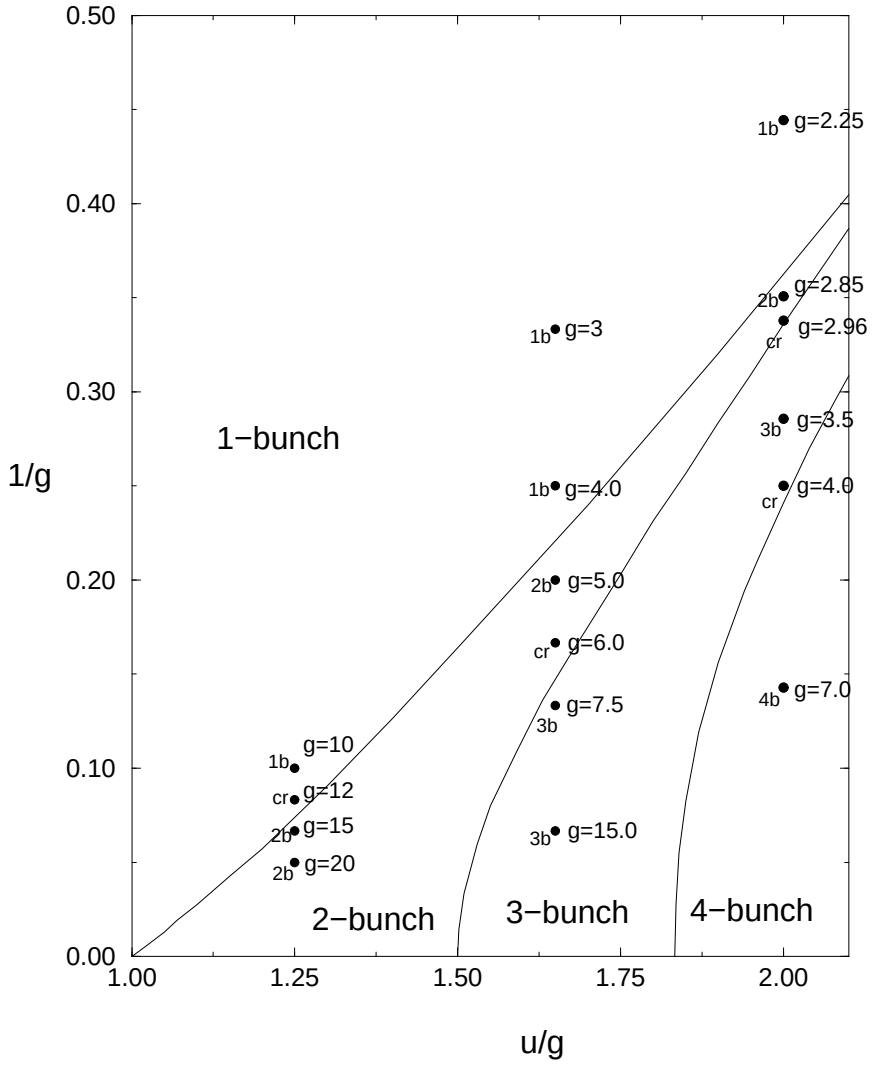
0.50
0.40
0.30
0.20
0.10
0.00
1/g
1.00
1.25
1.50
1.75
2.00
u/g
1−bunch
2−bunch
3−bunch
4−bunch
1b g=2.25
2b g=2.85
cr g=2.96
1b g=3
3b g=3.5
1b g=4.0
cr g=4.0
2b g=5.0
cr g=6.0
g=7.5
3b
4b g=7.0
1b g=10
cr g=12
2b g=15
2b g=20
3b g=15.0

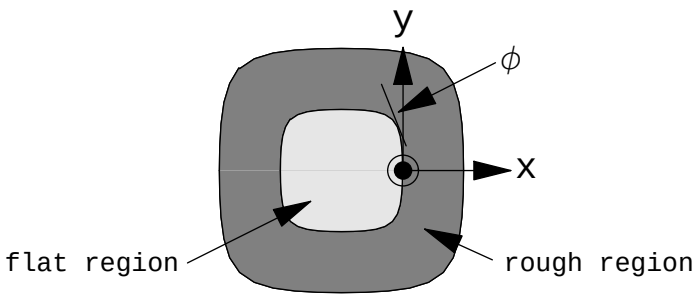
y
ϕ
x
flat region
rough region

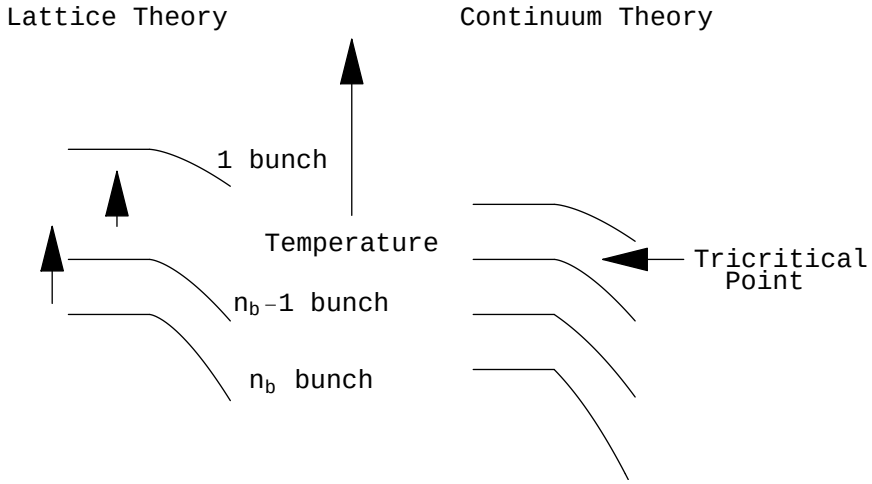
Lattice Theory
Continuum Theory
1 bunch
Temperature
Tricritical
Point
$n_b - 1$ bunch
n_b bunch